Pex20p of the Yeast *Yarrowia lipolytica* Is Required for the Oligomerization of Thiolase in the Cytosol and for Its Targeting to the Peroxisome

Vladimir I. Titorenko, Jennifer J. Smith, Rachel K. Szilard, and Richard A. Rachubinski

Department of Cell Biology and Anatomy, University of Alberta, Edmonton, Alberta T6G 2H7, Canada

Abstract. *Pex* mutants are defective in peroxisome assembly. In the *pex20-1* mutant strain of the yeast *Yarrowia lipolytica*, the peroxisomal matrix protein thiolase is mislocalized exclusively to the cytosol, whereas the import of other peroxisomal proteins is unaffected. The *PEX20* gene was isolated by functional complementation of the *pex20-1* strain and encodes a protein, Pex20p, of 424 amino acids (47,274 D). Despite its role in the peroxisomal import of thiolase, which is targeted by an amino-terminal peroxisomal targeting signal-2 (PTS2), Pex20p does not exhibit homology to Pex7p, which acts as the PTS2 receptor. Pex20p is mostly cytosolic, whereas 4–8% is associated with high-speed (200,000 *g*) pelletable peroxisomes. In the wild-type strain, all newly synthesized thiolase is associated with Pex20p in a heterotetrameric complex composed of two polypeptide chains of each protein. This association is independent of PTS2. Pex20p is required for both the oligomerization of thiolase in the cytosol and its targeting to the peroxisome. Our data suggest that monomeric Pex20p binds newly synthesized monomeric thiolase in the cytosol and promotes the formation of a heterotetrameric complex of these two proteins, which could further bind to the peroxisomal membrane. Translocation of the thiolase homodimer into the peroxisomal matrix would release Pex20p monomers back to the cytosol, thereby permitting a new cycle of binding-oligomerization-targeting-release for Pex20p and thiolase.

Key words: biogenesis • import • translocation • chaperone • cross-linking

Proteins targeted to the ER, mitochondria, and chloroplasts are translocated across the organellar membrane in an unfolded conformation, and folding and oligomerization of the proteins into active structures occurs within the organelle (McNew and Goodman, 1996; Schatz and Dobberstein, 1996). Maintenance of the unfolded, import-competent conformation is served by cytosolic chaperones that guide newly synthesized proteins from their site of synthesis at the ribosome to the target membrane (Hendrick and Hartl, 1993; Bukau et al., 1996; Hartl, 1996; Schatz and Dobberstein, 1996). However, recent evidence has shown that protein unfolding and disassembly are not prerequisites for import into the peroxisome. Completely folded polypeptides, oligomeric proteins, disulfide-bonded and chemically cross-linked proteins, and even proteins conjugated to 9-nm gold particles can be imported into the peroxisomal matrix (Glover et al., 1994*a*; McNew and Goodman, 1994; Walton et al., 1995; Elgersma et al., 1996; Häusler et al., 1996; Leiper et al., 1996; Lee et al., 1997). Whether the formation and maintenance of the folded, oligomeric import-competent conformation of peroxisomal proteins are assisted by a specialized set of cytosolic chaperones, or whether they occur spontaneously, remains unclear. Moreover, although numerous examples of peroxisomal import of oligomeric proteins have been reported (for reviews see Rachubinski and Subramani, 1995; McNew and Goodman, 1996; Subramani, 1998), this does not necessarily imply that all peroxisomal multimeric proteins enter the organelle strictly as preassembled oligomeric complexes. For example, alcohol oxidase monomers are imported into the matrix before the assembly of enzymatically active octamers (Bellion and Goodman, 1987; Waterham et al., 1997), and alanine:glyoxylate aminotransferase 1 can be imported with equal efficiency as a dimer or monomer (Leiper et al., 1996).

Two well-characterized peroxisomal targeting signals (PTS)[1] specify the sorting of matrix proteins to the or-

Address all correspondence to Richard A. Rachubinski, Department of Cell Biology and Anatomy, University of Alberta, Medical Sciences Building 5-14, Edmonton, Alberta T6G 2H7, Canada. Tel.: (403) 492-9868. Fax: (403) 492-9278. E-mail: rick.rachubinski@ualberta.ca

1. *Abbreviations used in this paper*: AOX, acyl-CoA oxidase; CAT, catalase; DSP, dithiobis(succinimidylproprionate); DSS, disuccinimidyl suberate; FUM, fumarase; G6PDH, glucose-6-phosphate dehydrogenase; HSP, high-speed (200,000 *g*) pelletable; ICL, isocitrate lyase; LSP, low-speed (20,000 *g*) pelletable; 20KgP, 20,000 *g* pellet; 20KgS, 20,000 *g* supernatant; 200KgP, 200,000 *g* pellet; 200KgS, 200,000 *g* supernatant (cytosol); MLS, malate synthase; PNS, postnuclear supernatant; PTS, peroxisomal targeting signal; THI, thiolase.

ganelle: a carboxyl-terminal tripeptide PTS1 and an amino-terminal nonapeptide PTS2 (for reviews see Purdue and Lazarow, 1994; Rachubinski and Subramani, 1995; Subramani, 1998). Import receptors and docking proteins for both PTS1- and PTS2-containing proteins have been identified (for reviews see Rachubinski and Subramani, 1995; Erdmann et al., 1997; Kunau, 1998; Subramani, 1998). The subcellular location of PTS1 and PTS2 receptors is a matter of debate and has been reported to be mainly cytosolic, partially peroxisomal, or even exclusively intraperoxisomal (Rachubinski and Subramani, 1995; Erdmann et al., 1997; Subramani, 1998). Accordingly, two models for PTS1 and PTS2 import receptor action have been proposed. One model proposes that peroxisomal import receptors are mobile, shuttling between the cytosol and the peroxisome (Marzioch et al., 1994; Dodt and Gould, 1996; Albertini et al., 1997; Elgersma et al., 1998), whereas the other proposes that the receptors act from inside the peroxisome to pull proteins in (Szilard et al., 1995; Zhang and Lazarow, 1995). Whether the accessibility of folded and oligomeric peroxisomal proteins to import receptors and/or their docking proteins could be served by specialized cytosolic proteins that stabilize the folded and oligomeric import-competent conformation and/or keep the PTS exposed for interaction with the import machineries is unknown. Here, we identify and characterize a cytosolic peroxin, Pex20p, of the yeast *Yarrowia lipolytica* that is required for the oligomerization of PTS2-containing thiolase (THI) in the cytosol and for its targeting to the peroxisome.

Materials and Methods

Strains, Culture Conditions, and Microbial Techniques

The *Y. lipolytica* strains used in this study are listed in Table I. The new nomenclature for peroxisome assembly genes and proteins has been used (Distel et al., 1996). Media, growth conditions, and genetic techniques for *Y. lipolytica* have been described (Nuttley et al., 1993; Szilard et al., 1995). Media components were as follows: (*a*) YEPD, 1% yeast extract, 2% peptone, 2% glucose; (*b*) YPBO, 0.3% yeast extract, 0.5% peptone, 0.5% K_2HPO_4, 0.5% KH_2PO_4, 1% Brij 35, 1% (wt/vol) oleic acid; (*c*) YNAS, 0.67% yeast nitrogen base without amino acids, 0.1% yeast extract, 18.2% sorbitol, 2% sodium acetate; (*d*) YND, 0.67% yeast nitrogen base without amino acids, 2% glucose; and (*e*) YNO, 0.67% yeast nitrogen base without amino acids, 0.05% (wt/vol) Tween 40, 0.1% (wt/vol) oleic acid. YNAS, YND, and YNO media were supplemented with leucine, uracil, lysine, and histidine, each at 50 μg/ml, as required. DNA manipulation and growth of *Escherichia coli* were performed as previously described (Ausubel et al., 1989).

Cloning, Sequencing, and Integrative Disruption of the PEX20 Gene

The *pex20-1* mutant was initially isolated from randomly mutagenized *Y. lipolytica* strain *E122* by screening for the inability to use oleic acid as a sole carbon source (Nuttley et al., 1993). The *PEX20* gene was isolated by functional complementation of the *pex20-1* strain using a *Y. lipolytica* genomic DNA library in the autonomously replicating *E. coli* shuttle vector pINA445 (Nuttley et al., 1993). Plasmid DNA was introduced into cells by electroporation (Nuttley et al., 1993). Leu^+ transformants recovered on YNAS agar plates were replica plated onto selective YNO agar plates and screened for restoration of their ability to use oleic acid as a sole carbon source. Total DNA was isolated from colonies that recovered growth and used to transform *E. coli* for plasmid recovery. Restriction fragments prepared from genomic inserts were subcloned and tested for their ability to functionally complement the *pex20-1* strain. Various restriction endonuclease fragments of the *PEX20* gene were cloned into the vectors pGEM5Zf (+) and pGEM7Zf (+) (Promega Corp., Madison, WI) for dideoxynucleotide sequencing of both strands. The deduced Pex20p amino acid sequence was compared with other known protein sequences using the GENEINFO (R) Blast Network Service (Blaster) of the National Center for Biotechnology Information (Bethesda, MD).

Targeted integrative disruption of the *PEX20* gene was performed with the *URA3* gene of *Y. lipolytica*. A 1.65-kbp SalI fragment containing the *URA3* gene was made blunt and ligated in reverse orientation into a plasmid containing the *PEX20* gene cut with NcoI and made blunt. In this way, 1,092 bp of the coding region and 2 bp of the 5′ untranslated region of the *PEX20* gene were replaced with the *URA3* gene flanked by 767 and 1,022 bp of the 5′ and 3′ regions, respectively, of the *PEX20* gene. This construct was cleaved with HindIII/SphI to liberate the *URA3* gene flanked by *PEX20* sequences. The resulting linear construct was used to transform *Y. lipolytica* strains *E122* and *22301-3* to uracil prototrophy. Ura^+ transformants that were unable to grow on YNO agar were further characterized by Southern blotting. *pex20::URA3* integrants were mated to each other, to wild-type strains, and to the *pex20-1* mutant strain, and the resulting diploids were subjected to complementation and random spore analyses (Nuttley et al., 1993).

Immunofluorescence and Electron Microscopy

Double-labeling, indirect immunofluorescence microscopy (Szilard et al., 1995), and electron microscopy (Goodman et al., 1990) were performed as described. For morphometric analysis of random electron microscopic sections of cells, 12 × 14-cm prints and 8 × 10-cm negatives of 35–40 cell sections of each strain at 24,000–29,000 magnification were scanned and converted to digitized images with an Apple Color OneScanner (Apple Computers Inc., Cupertino, CA) and Adobe Photoshop 3.0 software (Adobe Systems Inc., San Jose, CA). Quantitation of digitized images was performed using NIH Image 1.55 software (National Institutes of Health, Bethesda, MD). Relative area of peroxisome section (%) was calculated as "area of peroxisome section/area of cell section × 100". Peroxisomes were counted in electron micrographs, and data are expressed as the number of peroxisomes per μm^3 of cell section volume.

Organelle Fractionation and Isolation of Peroxisomes

The initial step in the subcellular fractionation of YPBO-grown cells was performed as described previously (Szilard et al., 1995) and included the differential centrifugation of lysed and homogenized spheroplasts at 1,000 *g* for 8 min at 4°C in a rotor (model JS13.1; Beckman Instrs., Inc., Palo Alto, CA) to yield a postnuclear supernatant (PNS) fraction. The PNS fraction was further subjected to differential centrifugation at 20,000 *g* for 30 min at 4°C in a rotor (model JS13.1; Beckman Instrs.) to yield pellet (20KgP) and supernatant (20KgS) fractions. The 20KgS fraction was further subfractionated by differential centrifugation at 200,000 *g* for 1 h at 4°C in a rotor (model TLA120.2; Beckman Instrs., Inc.) to yield pellet (200KgP) and supernatant (200KgS) fractions. The 200 KgP was further fractionated by flotation on a two-step sucrose gradient. Specifically, the 200 KgP was resuspended in 400 μl of 60% (wt/wt) sucrose in buffer H (5 mM MES, pH 5.5, 1 mM KCl, 0.5 mM EDTA, 0.1% [vol/vol] ethanol), overlaid with 2.3 ml of 50% (wt/wt) sucrose and 2.3 ml of 20% (wt/wt) sucrose (both in buffer H), and subjected to centrifugation in a rotor (model SW50.1; Beckman Instrs.) at 200,000 *g* for 18 h at 4°C. Gradients were fractionated from the bottom, and 18 fractions of ~270 μl each were collected. Protein extraction and protease protection analysis of different subcellular fractions were performed as described (Szilard et al., 1995).

Highly purified peroxisomes were isolated essentially as described (Titorenko et al., 1996). 4 vol of 0.5 M sucrose in buffer H were added to the peak peroxisomal fraction 4 recovered after isopycnic centrifugation on a discontinuous sucrose gradient. Peroxisomes were sedimented through a 150-μl cushion of 2 M sucrose in buffer H by centrifugation at 200,000 *g* for 20 min at 4°C in a TLA120.2 rotor. The resultant pellet was resuspended in buffer H containing 1 M sorbitol and was subjected to further centrifugation on a linear 20–60% (wt/wt) sucrose gradient (in buffer H) at 197,000 *g* for 18 h at 4°C in a rotor (model SW41Ti; Beckman Instrs., Inc.). Peak peroxisomal fraction 5 equilibrating at a density of 1.21 g/cm^3 was recovered, and peroxisomes were pelleted at 200,000 *g* for 20 min at 4°C in a TLA120.2 rotor, as described above. Pelleted peroxisomes were resuspended in 400 μl of 60% (wt/wt) sucrose in buffer H and subjected to flotation on a two-step sucrose gradient as described above. Peak peroxisomal fraction 11 was recovered and used for biochemical analyses. Perox-

isomes isolated by this multistep method were greater than 97% pure, as judged by the presence of marker proteins of other organelles.

Radiolabeling, Subcellular Fractionation, Chemical Cross-linking, and Immunoprecipitation

For pulse-chase experiments, YPBO-grown cells were pelleted at 10,000 *g* for 8 min at room temperature, washed three times with water, incubated in 50 mM potassium phosphate buffer, pH 7.5, containing 10 mM DTT for 10 min at 30°C, and repelleted at 10,000 *g* for 8 min at room temperature. Cells were resuspended at a concentration of 0.25 g/ml in 25 mM potassium phosphate buffer, pH 7.5, containing 0.55 M $MgSO_4$, and converted to spheroplasts by digestion at 30°C with Zymolyase 100T (ICN Biochemicals, Inc., Mississauga, Ontario, Canada) at 1 mg/ml of cells. Spheroplasts were harvested at 10,000 *g* for 8 min at room temperature and resuspended at a concentration of 6 OD_{600}/ml in YNO medium supplemented with 1 M sucrose. Spheroplasts were incubated for 90 min at 30°C, labeled with L-[^{35}S]methionine (ICN Biochemicals, Inc.) at 40 μCi/OD_{600} for 1.5 min or 3 min at 30°C, and chased with an equal volume of 2× YPBO medium supplemented with 1 M sucrose and 10 mM unlabeled L-methionine. Samples were taken at various times of chase, and spheroplasts were immediately pelleted in a rotor (model F241.5; Beckman Instrs., Inc.) at 20,000 *g* for 2 min at 4°C. All subsequent steps were performed at 4°C, and all solutions contained unlabeled L-methionine. Spheroplasts were resuspended in 150 μl of buffer H containing 1 M sorbitol and a mixture of protease inhibitors, as described previously (Szilard et al., 1995). In protease protection experiments, protease inhibitors were omitted. Spheroplasts were osmotically lysed by addition of 300 μl of buffer H containing 0.1 M sorbitol and protease inhibitors. Lysis was greater than 90%, as determined by microscopy and enzymatic assay of the cytosolic marker G6PDH. The original osmolarity was reestablished by addition of 300 μl of buffer H containing 1.9 M sorbitol and protease inhibitors. The lysate was subjected to centrifugation at 1,000 *g* for 3 min at 4°C in a rotor (model F241.5; Beckman Instrs., Inc.) to yield a PNS fraction. The PNS fraction was loaded onto a 150-μl cushion of 1.2 M sucrose in buffer H containing protease inhibitors and subjected to centrifugation at 20,000 *g* for 20 min at 4°C in a rotor (model TLA120.2; Beckman Instrs., Inc.) to yield pellet (20KgP) and supernatant (20KgS) fractions. The 20KgS fraction was further sedimented through a 150-μl cushion of 1.2 M sucrose in buffer H containing protease inhibitors at 200,000 *g* for 20 min at 4°C in a rotor (model TLA120.2; Beckman Instrs., Inc.) to yield pellet (200KgP) and supernatant (200KgS) fractions. Immunoprecipitation under native conditions was performed by immunoaffinity chromatography with antibodies covalently coupled to protein A–Sepharose (Pharmacia LKB Biotechnology, Piscataway, NJ), as described previously (Szilard et al., 1995). For immunoprecipitation under denaturing conditions, SDS was added to 2%, and samples were warmed at 65°C for 10 min. Samples were allowed to cool to room temperature, and 4 vol of 60 mM Tris-HCl, pH 7.4, buffer containing 1.25% (vol/vol) Triton X-100, 190 mM NaCl, and 6 mM EDTA were added. Samples were subsequently processed for immunoprecipitation, as described (Franzusoff et al., 1991).

Chemical cross-linking of proteins was performed using dithiobis(succinimidylpropionate) (DSP) and disuccinimidyl suberate (DSS) (Pierce Chemical Co., Rockford, IL), essentially as described (Sanders et al., 1992; Marshall et al., 1996). Highly purified peroxisomes or the 200 KgP fraction were lysed in 20 mM sodium phosphate buffer, pH 7.5, containing 150 mM NaCl. Lysates were clarified by centrifugation at 200,000 *g* for 20 min at 4°C in a rotor (model TLA120.2; Beckman Instrs., Inc.), and the resultant supernatants were used for chemical cross-linking. Sodium phosphate buffer, pH 7.5, and NaCl were added to the supernatants to final concentrations of 20 and 150 mM, respectively. Cross-linking with DSP or DSS was initiated by the addition of cross-linker (50 mM stock in DMSO) and continued for 1 h at 4°C. Cross-linking was quenched by addition of 0.1 vol of 1 M Tris-HCl, pH 7.5, and incubation for 30 min at 4°C. SDS was added to 1.25%, and samples were warmed at 65°C for 20 min and then cooled to room temperature. 4 vol of 60 mM Tris-HCl, pH 7.4, 1.25% (vol/vol) Triton X-100, 190 mM NaCl, and 6 mM EDTA were added to the cooled samples, which were then subjected to immunoprecipitation, as described (Franzusoff et al., 1991). All immunoprecipitated samples were analyzed by SDS-PAGE under reducing or nonreducing conditions, i.e., with or without DTT in the sample buffer, respectively. Gels were treated with 22.2% 2,5-diphenyloxazole in either DMSO or glacial acetic acid (Coligan et al., 1995), dried, and then exposed to preflashed Kodak X-Omat AR X-ray film (Eastman-Kodak Co., Rochester, NY) at −80°C with intensifying screens.

Antibodies

Antibodies to Pex20p were raised in guinea pig and rabbit against a maltose-binding protein-Pex20p fusion, as described previously (Eitzen et al., 1995). To produce antibodies to Pex20p, the entire open reading frame of the *PEX20* gene was amplified by PCR and inserted into pMAL-c2 (New England BioLabs, Beverly, MA) in-frame and downstream of the open reading frame encoding the maltose-binding protein (Eitzen et al., 1995).

Guinea pig polyclonal antibodies to *Y. lipolytica* isocitrate lyase (ICL), thiolase (THI), Pex2p, Pex5p, and Pex16p and to *Saccharomyces cerevisiae* acyl-CoA oxidase (AOX); and rabbit polyclonal anti-SKL antibodies have been described (Szilard et al., 1995; Eitzen et al., 1996, 1997). Rabbit polyclonal antibodies to *S. cerevisiae* malate synthase (MLS) (Eitzen et al., 1996) and to *Y. lipolytica* Sls1p (Boisramé et al., 1996), Kar2p (Titorenko et al., 1997) and Sec14p (Lopez et al., 1994) were described previously. Anti-MLS antibodies were kindly provided by A. Hartig (Institute of Biochemistry and Molecular Cell Biology, Vienna, Austria). Anti-Sls1p and anti-Sec14p antibodies were generous gifts of C. Gaillardin (Institut National Agronomique Paris-Grignon, Thiveral-Grignon, France). Rabbit polyclonal antibody A-9521 specific for *S. cerevisiae* glucose-6-phosphate dehydrogenase (G6PDH) was from Sigma Chemical Co. (St. Louis, MO).

Other Methods

Whole cell lysates were prepared as described (Goodman et al., 1990). The progressive permeabilization of yeast membranes with digitonin was performed as described (Zhang et al., 1993). In vitro coupled transcription/translation of the *PEX20* gene was performed using the TNT T7 Quick-Coupled Transcription/Translation System (Promega Corp.). Blot overlay (Radu et al., 1995), including the denaturation/renaturation of transferred proteins by treatment with guanidinium chloride, followed by multistep dilution with water (Dingwall et al., 1995) and elution of bound proteins with urea (Radu et al., 1995), were performed according to established procedures. Enzymatic activities of catalase and cytochrome *c* oxidase (Szilard et al., 1995); NADPH:cytochrome *c* reductase, α-mannosidase, and vanadate-sensitive plasma membrane ATPase (Roberts et al., 1991); guanosine diphosphatase (Abeijon et al., 1989); fumarase (Smith et al., 1997); and alkaline phosphatase (Thieringer et al., 1991); and thiolase (Glover et al., 1994*b*) were determined by established methods. Inorganic phosphate liberated in assays of the activities of guanosine diphosphatase and vanadate-sensitive plasma membrane ATPase was measured as described (Lanzetta et al., 1979). Southern blot analysis (Ausubel et al., 1989), SDS-PAGE (Laemmli, 1970), and immunoblotting using a semi-dry electrophoretic transfer system (model ET-20; Tyler Research Instruments, Edmonton, Alberta, Canada) (Kyhse-Andersen, 1984) were performed as described. Antigen–antibody complexes were detected by enhanced chemiluminescence (Amersham Life Sciences, Oakville, Ontario, Canada). Quantitation of immunoblots was performed as described (Szilard et al., 1995).

Results

Isolation and Characterization of the PEX20 Gene

We have previously reported the isolation of *Y. lipolytica* mutants that are unable to use oleic acid as a sole carbon source (Nuttley et al., 1993). This collection of ole$^-$ mutants was screened by indirect immunofluorescence using antibodies to PTS1, to the peroxisomal matrix protein THI, which is targeted by PTS2, and to the peroxisomal membrane protein Pex2p. One mutant strain, *pex20-1*, exhibited a punctate pattern characteristic of peroxisomes when stained with either anti-PTS1 or anti-Pex2p antibodies (see below). However, unlike wild-type cells, a diffuse pattern of staining was seen with anti-THI antibodies, indicating that the *pex20-1* mutant strain is impaired in the import of THI into peroxisomes.

The *PEX20* gene was isolated by functional complementation of the *pex20-1* strain. Of the 2×10^4 Leu$^+$ transformants screened, five strains were found to have re-

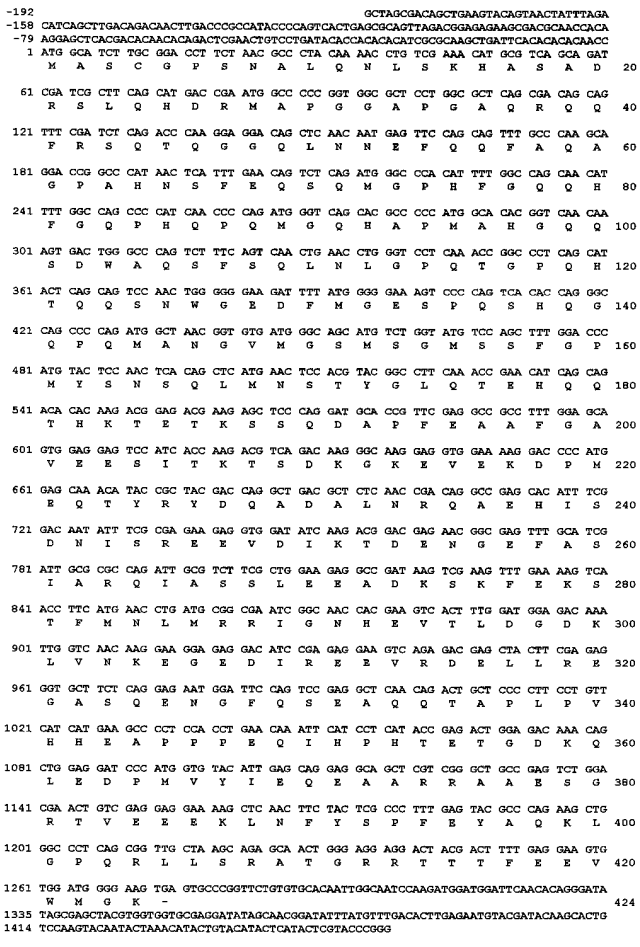

Figure 1. Nucleotide sequence of the *PEX20* gene and deduced amino acid sequence of Pex20p. These sequence data are available from EMBL/GeneBank/DDBJ under accession number AF054613.

stored growth on oleic acid. The complementing plasmids were recovered after transformation of *E. coli*. Restriction map analysis showed that all five complementing plasmids shared a 5.8-kbp region. Restriction fragments from this region were subcloned and tested for their ability to functionally complement the *pex20-1* strain. The minimum complementing fragment was localized to a 2.9-kbp HindIII/BamHI restriction fragment. Sequencing this fragment revealed a 1,272-bp open reading frame encoding a 424-amino acid protein, Pex20p, with a predicted molecular weight of 47,274 (Fig. 1). Pex20p shows 16.3 to 28.1% identity to Pex5p peroxins of yeast and mammals, including *Y. lipolytica* Pex5p, but does not contain tetratricopeptide repeat motifs. Pex5p peroxins function as PTS1 import receptors (Erdmann et al., 1997). However, Pex20p is not required for the import of PTS1 proteins (see below). Despite its role in the peroxisomal import of PTS2-containing THI, Pex20p does not exhibit homology to yeast or human Pex7p peroxins, which act as import receptors for PTS2-containing proteins (Erdmann et al., 1997).

The putative *PEX20* gene was disrupted by targeted integration of the *Y. lipolytica URA3* gene to create the strains *pex20KO-1A* and *pex20KO-2B* in the *A* and *B* mating types, respectively (Table I). Strains containing a disrupted *PEX20* gene were unable to grow on oleic acid and had the morphological and biochemical characteristics of the original *pex20-1* strain (see below). The diploid strain *D1-20* from the mating of wild-type strain *E122* to strain *pex20KO-2B*, and the diploid strains *D2-20* and *D3-20* from the mating of strains *pex20KO-1A* and *pex20-1*, respectively, to wild-type strain *22301-3* (Table I), could grow on oleic acid-containing medium, demonstrating the recessive nature of the *pex20-1*, *pex20KO-1A,* and *pex20KO-2B* mutations. The diploid strain *D4-20* from the mating of the original *pex20-1* mutant strain to strain *pex20KO-2B*, and the diploid strain *D5-20* from the mating of the *pex20KO-1A* strain to strain *pex20KO-2B* (Table I), were unable to grow on oleic acid-containing medium. Random spore analysis of the diploid strains *D1-20* and *D2-20* showed monogenic segregation for both Ura$^+$ and ole$^-$ phenotypes, whereas the *URA3* gene invariably cosegregated with the ole$^-$ phenotype. Random spore analysis of the diploid strain *D4-20* and of the diploid strain *D5-20* revealed no meiotic segregants with a recombinant ole$^+$ phenotype. Taken together, these data indicate that the authentic *PEX20* gene had been cloned.

Subcellular Localization and Intracellular Trafficking of Pex20p

Antibodies to Pex20p specifically recognized an ~60-kD polypeptide in whole cell lysates prepared from the wild-type strain, but not from the *pex20-1* or *pex20KO* mutant strains (Fig. 2 *A*). The difference between the predicted molecular weight of Pex20p (47,274 D) and its empirical molecular weight (~60,000 D), as determined from SDS-PAGE, is an intrinsic feature of this protein. Indeed, in vitro coupled transcription/translation of the *PEX20* gene yielded a polypeptide that comigrated identically with in vivo synthesized Pex20p on SDS-PAGE (data not shown). Why Pex20p shows reduced electrophoretic mobility on SDS-PAGE is unknown, but may be due to the large number of acidic amino acids (14.4%) present in Pex20p.

Table I. Yarrowia lipolytica Strains Used in This Study

Strain	Genotype
*E122**	*MATA, ura3-302, leu2-270, lys8-11*
*22301-3**	*MATB, ura3-302, leu2-270, his1*
pex5KO‡	*MATA, ura3-302, leu2-270, lys8-11, pex5::LEU2*
pex20-1§	*MATA, ura3-302, leu2-270, lys8-11, pex20-1*
pex20KO-1A§	*MATA, ura3-302, leu2-270, lys8-11, pex20::URA3*
pex20KO-2B§	*MATB, ura3-302, leu2-270, his1, pex20::URA3*
D1-20§	*MATA/MATB, ura3-302/ura3-302, leu2-270/leu2-270, lys8-11/+, +his1, +/pex20::URA3*
D2-20§	*MATB/MATA, ura3-302/ura3-302, leu2-270/leu2-270, +/lys8-11, his1/+, +/pex20::URA3*
D3-20§	*MATB/MATA, ura3-302/ura3-302, leu2-270/ leu2-270, +/lys8-11, his1/+, +/pex20-1*
D4-20§	*MATA/MATB, ura3-302/ura3-302, leu2-270/leu2-270, lys8-11/+, +/his1, pex20-1/pex20::URA3*
D5-20§	*MATA/MATB, ura3-302/ura3-302, leu2-270/leu2-270, lys8-11/+, +/his1, pex20::URA3/pex20::URA3*

*C. Gaillardin (Institut National Agronomique Paris-Grignon) Thiverval-Grignon, France.
‡Szilard et al., 1995.
§This study.

Synthesis of Pex20p is induced by growth of *Y. lipolytica* on oleic acid (Fig. 2 *B*). A small amount of Pex20p was present in wild-type cells grown in glucose-containing medium. Shifting cells to oleic acid-containing medium caused an increase in the level of Pex20p, which reached levels ~24 times that found in glucose-grown cells 8 h after the shift (Fig. 2 *B*).

In wild-type cells, most (98 ± 8%) of Pex20p localized to the cytosol, whereas 6 ± 2% associated with a high-speed (200,000 *g*) pelletable organellar fraction (200KgP) (Fig. 2 *C*) enriched for high-speed pelletable (HSP) peroxisomes (see below). Cytosolic G6PDH was not detected in the 200KgP isolated under these fractionation conditions (data not shown). No Pex20p was detected in a low-speed (20,000 *g*) organellar fraction (20KgP) (Fig. 2 *C*) enriched for low-speed pelletable (LSP) peroxisomes (see below). The predominantly cytosolic location of Pex20p was confirmed by two additional approaches. Spheroplasts of oleic

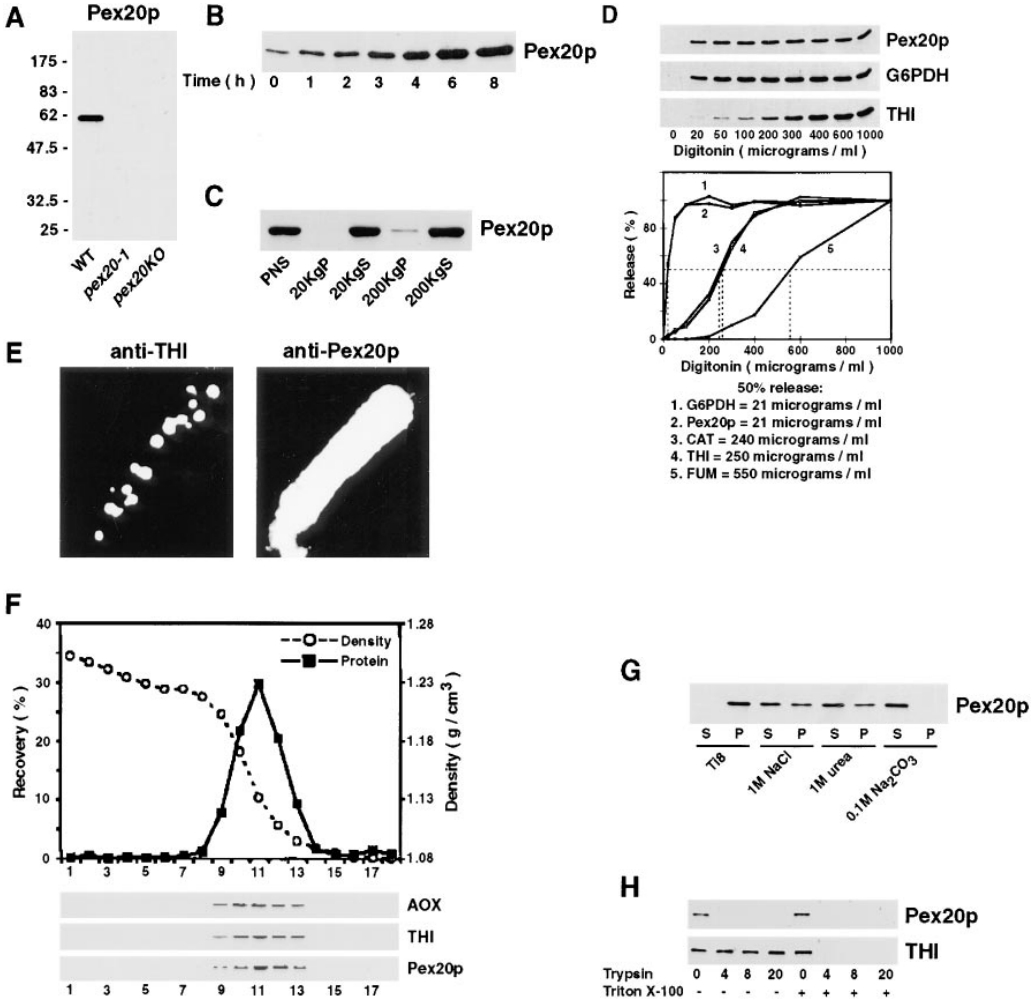

Figure 2. Subcellular localization and regulation of synthesis of Pex20p. (*A*) Immunoblot analysis of whole cell lysates (3×10^8 cells) of wild-type strain *E122* (*WT*), and *pex20-1* and *pex20KO* mutant strains probed with anti-Pex20p antibodies. Strains were grown in YPBO for 9 h. (*B*) Wild-type strain *E122* was grown in YEPD until the cell titer was 6.0×10^7 cells/ml. Cells were transferred to YPBO and incubated at 30°C. Equal aliquots of cells were taken at the times indicated. The levels of Pex20p in whole cell lysates were determined by immunoblotting. Blots were probed with anti-Pex20p antibodies. (*C*) Equal portions of the indicated subcellular fractions from YPBO-grown wild-type cells were separated by SDS-PAGE and analyzed by immunoblotting with anti-Pex20p antibodies. (*D*) Release of intracellular proteins by progressive digitonin titration of YPBO-grown wild-type cells. Aliquots of spheroplasts were incubated with different concentrations of digitonin for 30 min at 4°C and then subjected to centrifugation at 20,000 *g* for 10 min at 4°C. Supernatants were analyzed for the release of proteins. The activities of the peroxisomal enzyme catalase (*CAT*) and the mitochondrial enzyme fumarase (*FUM*) were determined. The cytosolic marker G6PDH, the peroxisomal matrix marker THI, and Pex20p were determined by immunoblotting. Immunoblots were scanned densitometrically, and protein levels were quantitated. The amount of each protein released to the supernatant was normalized to the amount of that protein released to the supernatant at a concentration of 1,000 μg digitonin/ml. (*E*) Double-labeling, indirect immunofluorescence analysis of YPBO-grown wild-type cells using rabbit anti-THI and guinea pig anti-Pex20p primary antibodies. Primary antibodies were detected with fluorescein-conjugated goat anti–rabbit IgG and rhodamine-conjugated donkey anti–guinea pig IgG secondary antibodies. (*F*) The 200KgP fraction of the wild-type strain *E122* grown in YPBO for 9 h was subjected to flotation on a two-step sucrose gradient. Sucrose density (g/cm^3) and percent recovery of loaded protein in gradient fractions are presented. Equal volumes of gradient fractions were analyzed by immunoblotting with anti-AOX, anti-THI, and anti-Pex20p antibodies. (*G*) Equal portions of the 200KgP fraction of the wild-type strain *E122* grown in YPBO for 9 h were treated with one of Ti8 buffer (10 mM Tris-HCl, pH 8.0, 5 mM EDTA, 1 mM PMSF, 1 μg leupeptin/ml, 1 μg pepstatin/ml, 1 μg aprotinin/ml), 1 M NaCl, 1 M urea or 0.1 M Na_2CO_3. After incubation on ice for 45 min, samples were separated into supernatant (*S*) and pellet (*P*) fractions by centrifugation at 200,000 *g* for 1 h at 4°C, and then subjected to immunoblot analysis with anti-Pex20p antibodies. (*H*) Protease protection analysis. The 200KgP fraction (60 μg of protein) of the wild-type strain *E122* grown in YPBO for 9 h was incubated with 0, 4, 8, or 20 μg trypsin in the absence (−) or presence (+) of 1.0% (vol/vol) Triton X-100 for 60 min on ice. Reactions were terminated by addition of TCA to 10%. Equal portions of the samples were subjected to immunoblot analysis with anti-Pex20p and anti-THI antibodies.

acid-grown wild-type cells were permeabilized by incubation with increasing amounts of digitonin, and the subsequent leakage of Pex20p and marker proteins from the cells was quantitated. Pex20p was released at low concentrations of digitonin, as was the cytosolic marker G6PDH. 50% release of both Pex20p and G6PDH was observed at 21 μg digitonin/ml (Fig. 2 *D*). The peroxisomal matrix proteins CAT and THI, and the mitochondrial matrix protein fumarase (*FUM*), were released at much higher concentrations of digitonin (Fig. 2 *D*). Double-labeling, indirect immunofluorescence analysis of wild-type cells grown in oleic acid-containing medium with anti-THI antibodies yielded a punctate pattern of staining characteristic of peroxisomes (Fig. 2 *E*). In contrast, a diffuse pattern of staining was observed with anti-Pex20p antibodies (Fig. 2 *E*), indicating that most Pex20p is localized to the cytosol in wild-type cells.

Pex20p localized to the 200KgP is present in membrane-associated form and is not due to aggregation. Flotation of the 200KgP from wild-type cells on a two-step sucrose gradient revealed that Pex20p, similar to the matrix proteins AOX and THI, floated out of the most dense sucrose and concentrated at the interface between 50 and 20% sucrose (Fig. 2 *F*). The distribution of Pex20p around peak fraction 11 coincided with the distributions of AOX and THI (Fig. 2 *F*), suggesting that Pex20p is localized to HSP peroxisomes. Further fractionation of the 200KgP on additional gradients showed that Pex20p cofractionated with the peroxisomal proteins AOX, THI, MLS, Pex2p, and Pex16p, but not with markers of the ER, Golgi, vacuole, or plasma membrane (data not shown). Together, these data indicate that Pex20p is localized to HSP peroxisomes and is not associated with any other organelle. Extraction of the 200KgP-associated form of Pex20p with various solubilizing agents showed that Pex20p fractionated as a peripheral membrane protein that was solubilized to a significant extent by either 1 M NaCl or 1 M urea or completely by 0.1 M Na_2CO_3, pH 11 (Fig. 2 *G*). Protease protection experiments revealed that the 200KgP-associated form of Pex20p was sensitive to trypsin digestion even in the absence of Triton X-100, whereas the peroxisomal matrix protein THI was degraded by trypsin only when the membranes of the 200KgP-associated organelles were disrupted by the detergent (Fig. 2 *H*). Taken together, these data indicate that in wild-type cells, the 200KgP-associated form of Pex20p is a peripheral membrane protein associated with the cytosolic surface of HSP peroxisomes.

Intracellular trafficking of Pex20p was studied by immunoprecipitation of pulse-labeled and chased Pex20p from the 20KgP, 200KgP, and 200KgS (cytosolic) fractions of oleic acid-grown wild-type cells. At 0 min of chase, all Pex20p was found in the cytosol (Fig. 3 *A*). By 3 min of chase, a minor portion of Pex20p (10% of the total pool) was chased to the 200KgP enriched for HSP peroxisomes. By 10 min of chase, the 200KgP-associated Pex20p reached its maximal level of 26% of the total pool of pulse-labeled Pex20p (Fig. 3 *A*). After 10 min of chase, the level of 200KgP-associated Pex20p gradually decreased and, by 90 min of chase, reached 55% of its maximal level (Fig. 3 *A*). No Pex20p was chased to the 20KgP (Fig. 3 *A*), enriched for LSP peroxisomes. All pulse-labeled Pex20p chased to the 200KgP was sensitive to trypsin digestion even in the absence of Triton X-100 (Fig. 3 *B*) and, therefore, was associated with the cytosolic surface of HSP peroxisomes present in the 200KgP. These data suggest that a minor fraction (not more than 26%) of newly synthesized Pex20p is targeted from the cytosol to the outer surface of HSP peroxisomes with a half-time of 4 min. These results are consistent with a model in which Pex20p shuttles between the cytosol and the cytosolic surface of HSP peroxisomes; however, we cannot rule out the possibility that the decrease in the levels of pulse-labeled Pex20p in the 200KgP over time is due to its turnover in this fraction.

Ultrastructure of the Wild-Type and pex20 Mutant Strains

We assessed the effects of mutations in the *PEX20* gene on the size and number of peroxisomes in oleic acid-grown cells. EM and morphometric analysis showed that in wild-type cells, 36.2 ± 0.8% of all peroxisomes had relative areas of peroxisome section from 1.01–1.5%, whereas very small peroxisomes with relative areas of peroxisome section from 0.05 to 0.2% were much less abundant (5.3 ± 0.2% of all peroxisomes) (Fig. 4). Neither the *pex20-1* nor the *pex20KO* mutant showed a significant decrease in the percentage of peroxisomes with relative areas of peroxisome section from 0.21 to 3.0%, but both mutants showed 3.5- to 4.9-fold increases in the percentage of very small peroxisomes with relative areas of peroxisome section from 0.05 to 0.2% (Fig. 4). This increased percentage in small peroxisomes in mutant cells was due to a large increase in their number per cell rather than to a reduction in the number of large peroxisomes. Indeed, mutations in the *PEX20* gene did not significantly decrease the number of peroxisomes with relative areas of peroxisome section greater than 0.2% (Fig. 4). Rather, the *pex20-1* and *pex20KO* mutations led to 3.5- to 4.5-fold increases in the number of very small peroxisomes with relative areas of peroxisome section less than 0.2% (7.6 ± 0.8 and 9.9 ± 1.0 peroxisomes per μm^3 of cell section volume, respectively)

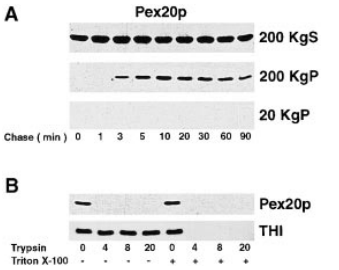

Figure 3. Trafficking of Pex20p. (*A*) Wild-type strain *E122* grown in YPBO for 9 h was pulse-labeled with L-[^{35}S]methionine and chased with unlabeled L-methionine. Samples were taken at the indicated times after chase. Cells were subjected to subcellular fractionation to yield 20KgP, 200KgP, and 200KgS (cytosolic) fractions. Pex20p was immunoprecipitated from the fractions. Immunoprecipitates were resolved by SDS-PAGE and visualized by fluorography. (*B*) Equal portions of the 200KgP fraction isolated from YPBO-grown wild-type cells pulse-labeled with L-[^{35}S]methionine and chased for 5 min with unlabeled L-methionine, were incubated with 0, 4, 8, or 20 μg trypsin in the absence (−) or presence (+) of 1.0% (vol/vol) Triton X-100 for 60 min on ice. Reactions were terminated by addition of TCA to 10%. Samples were subjected to immunoprecipitation with anti-Pex20p or anti-THI antibodies, and immunoprecipitates were resolved by SDS-PAGE and then visualized by fluorography.

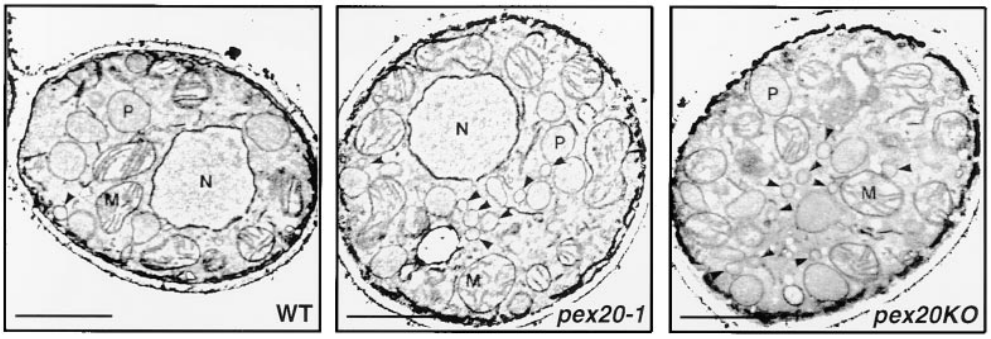

Figure 4. Ultrastructure of wild-type and *pex20* mutant strains. Wild-type strain *E122* (*WT*) and mutant strains *pex20-1* and *pex20KO* grown for 9 h in YPBO were fixed in $KMnO_4$ and processed for EM. *P*, peroxisome; *M*, mitochondrion; *N*, nucleus. *Arrowheads*, peroxisomes having a "relative area of peroxisome section (%)" of 0.05–0.2%. Bar, 1 μm.

vis-à-vis their number in wild-type cells (2.2 ± 0.3 peroxisomes per μm^3 of cell section volume). Biochemical results demonstrating the selective enrichment of MLS, CAT, Pex2p, and Pex16p in HSP peroxisomes in *pex20-1* and *pex20KO* cells (Fig. 5), combined with immunofluorescence data showing an accumulation of punctate structures decorated by anti-MLS or anti-Pex2p antibodies but not anti-SKL antibodies in these cells (see Fig. 8 *A*), strengthened the interpretation of EM data showing a large increase in the number of small peroxisomes in the *pex20-1* and *pex20KO* mutants.

Mutations in the PEX20 Gene Selectively Affect the Import of Thiolase into Peroxisomes

Subcellular fractionation of wild-type cells grown in oleic acid-containing medium showed that from 82 to 92% of peroxisomal matrix (AOX, 62- and 64-kD anti-SKL reactive proteins, ICL, CAT, MLS, and THI) and membrane (Pex2p and Pex16p) proteins was associated with a LSP organellar fraction (20KgP), whereas from 10 to 23% was localized to a HSP fraction (200KgP) (Fig. 5). Matrix proteins and the intraperoxisomal peripheral membrane protein Pex16p localized to the 20KgP and 200KgP of wild-type cells were resistant to exogenously added protease (trypsin) in the absence of Triton X-100 and were therefore in membrane-enclosed structures (data not shown). In contrast, in *pex20-1* and *pex20KO* cells, THI was found exclusively in the 200KgS (cytosolic) fraction (Fig. 5) and was accessible to external protease (data not shown). No other peroxisomal matrix or membrane protein was mislocalized to the cytosol in *pex20* mutants (Fig. 5). However, mutations in the *PEX20* gene altered the relative distributions of CAT, MLS, Pex2p, and Pex16p between the 20KgP and 200KgP fractions. In wild-type cells, 82–87% of these four proteins was found in the 20KgP, whereas 8–21% was associated with 200KgP (Fig. 5). In *pex20-1* and *pex20KO* cells, 44–74% of CAT, MLS, Pex2p, and Pex16p was localized to the 200KgP, whereas 30–45% was found in the 20KgP (Fig. 5). Neither the *pex20-1* nor the *pex20KO* mutation altered the relative distributions of AOX, 62-kD SKL, 64-kD SKL and ICL between the 20KgP and 200KgP fractions (Fig. 5).

Pulse-chase labeling and immunoprecipitation of proteins from the 20KgP, 200KgP, and 200KgS (cytosolic) fractions showed that in wild-type cells, peroxisomal matrix proteins moved from the cytosol to the 200KgP fraction and from there to the 20KgP fraction (Fig. 6 *A*, data

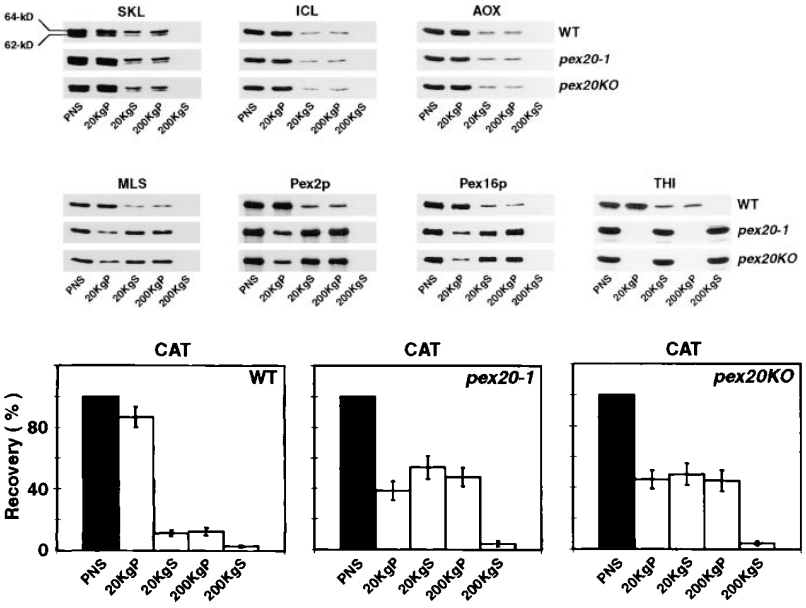

Figure 5. Subcellular localization of peroxisomal matrix and membrane proteins in wild-type and *pex20* mutant strains. The recoveries of the matrix proteins AOX, 62-kD SKL, 64-kD SKL, ICL, CAT, MLS, and THI, and of the membrane proteins Pex2p and Pex16p, in different subcellular fractions of the wild-type strain *E122* (*WT*) and of the mutant strains *pex20-1* and *pex20KO* are presented. Strains were grown for 9 h in YPBO and subjected to subcellular fractionation. Equal portions of the PNS, 20KgP, 20KgS, 200KgP, and 200KgS were analyzed by immunoblotting with antibodies to the indicated proteins. The activity of CAT was assayed enzymatically. Values for CAT activity in the 20KgP, 20KgS, 200KgP, and 200KgS fractions are relative to CAT activity in the PNS fraction of the indicated strain. Values for enzymatic activities are the means ± SD from three independent experiments.

for AOX, MLS and THI; data for 62-kD SKL, 64 kD-SKL, and ICL not shown). Furthermore, in wild-type cells, the peroxisomal membrane proteins Pex2p and Pex16p were initially targeted to the 20KgP, presumably to a subpopulation of ER-derived membranes that accumulates in this fraction (Titorenko and Rachubinski, 1998), and were subsequently chased to the 200KgP and from there to the 20KgP (Fig. 6 *A*, data for Pex2p; data for Pex16p not shown). Mutations in the *PEX20* gene selectively abolished the targeting of THI from the cytosol to the 200KgP (Fig. 6 *A* and *B*, compare data for THI). All THI accumulating in the cytosol of the *pex20-1* and *pex20KO* mutant strains was present as the 47-kD precursor form (data not shown). In wild-type cells, maturation of the THI precursor to the 45-kD mature form occurred in the 200KgP (Fig. 6 *C*).

In contrast to the targeting defect for THI, the rates and efficiencies of targeting from cytosol to the 200KgP of other peroxisomal matrix and membrane proteins were unaffected in *pex20* mutant strains (Fig. 6 *A* and *B,* compare half-times for the targeting of AOX, MLS, and Pex2p from the 200KgS to the 200KgP; data for 62-kD SKL, 64-kD SKL, and ICL not shown). The *pex20-1* and *pex20KO* mutations also did not affect the rates and efficiencies of transit of AOX, 62-kD SKL, 64-kD SKL and ICL from the 200KgP to the 20KgP (Fig. 6 *A* and *B*, compare data for AOX; data for 62-kD SKL, 64-kD SKL, and ICL not shown). However, mutations in the *PEX20* gene significantly decreased the rates and efficiencies of transit of MLS, Pex2p, and Pex16p from the 200KgP to the 20KgP (Fig. 6, *A* and *B*, compare data for MLS and Pex2p; data for Pex16p not shown).

The accumulation of thiolase in the cytosol and the differential transit of two subsets of peroxisomal proteins from the 200KgP to the 20KgP in *pex20-1* and *pex20KO* mutants should lead to the accumulation in these mutants of LSP peroxisomes that completely lack THI, are partially depleted of MLS, Pex2p, and Pex16p, but contain wild-type amounts of AOX, 62-kD SKL, and 64-kD SKL and ICL. To test this prediction, the 20KgP fractions from oleic-acid grown wild-type, *pex20-1,* and *pex20KO* cells were separated by isopycnic centrifugation on a discontinuous sucrose gradient (Fig. 7). In the wild-type strain, all peroxisomal proteins were primarily in fractions 1–7,

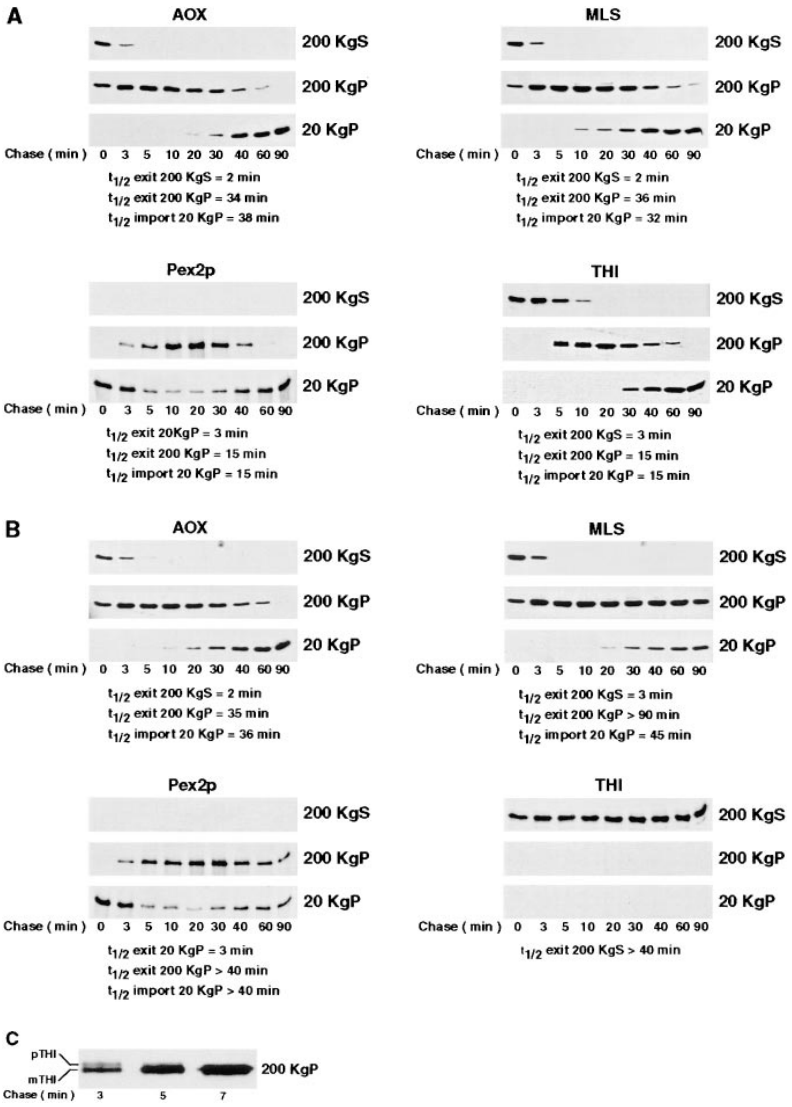

Figure 6. Trafficking of peroxisomal matrix and membrane proteins in wild-type and *pex20KO* cells. Wild-type strain *E122* (*WT*) (*A* and *C*) and mutant strain *pex20KO* (*B*) grown in YPBO for 9 h were pulse labeled with L-[^{35}S]methionine and chased with unlabeled L-methionine. Samples were taken at the indicated times after chase. Cells were subjected to subcellular fractionation to yield 20KgP, 200KgP, and 200KgS (cytosolic) fractions. AOX, MLS, Pex2p, and THI were immunoprecipitated from the fractions. Immunoprecipitates were resolved by SDS-PAGE and visualized by fluorography. Fluorograms were quantitated by densitometry. The maximal level of a protein in a particular fraction is set at 100%. Half-times for the exit from, and for the import into, a particular fraction by a protein in either wild-type or *pex20KO* cells were calculated. (*C*) Conversion of the precursor form of THI (*pTHI*) to the mature form of THI (*mTHI*) occurs in the 200KgP fraction of wild-type cells. 200KgP fractions were isolated from wild-type cells subjected to pulse labeling with L-[^{35}S]methionine and chase with unlabeled L-methionine. pTHI and mTHI were immunoprecipitated from the 200KgP fractions isolated from cells harvested at the indicated times after chase, resolved by SDS-PAGE, and then visualized by fluorography.

peaking in fraction 4 at a density of 1.21 g/cm^3 (Fig. 7, *left panel*). In the *pex20-1* and *pex20KO* mutants, all peroxisomal proteins, except THI, also peaked in fraction 4 at the same density (Fig. 7, *middle* and *right panels*, respectively). No THI was recovered in gradient fractions isolated from *pex20-1* and *pex20KO* cells (Fig. 7, *middle* and *right panels*). Therefore, LSP peroxisomes accumulating in *pex20* mutants have the same buoyant density as LSP peroxisomes present in wild-type cells, but they lack THI. AOX, 62-kD SKL, and 64-kD SKL, and ICL were present in LSP peroxisomes of the *pex20-1* and *pex20KO* strains at levels comparable to those found in LSP peroxisomes of the wild-type strain. On the other hand, the levels of MLS, CAT, Pex2p, and Pex16p in LSP peroxisomes of the *pex20-1* and *pex20KO* strains were 37–57% of their levels in LSP peroxisomes of the wild-type strain. Again, no THI was found in LSP peroxisomes of the *pex20* mutant strains.

In immunofluorescence analysis, oleic acid-grown wild-type cells showed a punctate pattern of staining characteristic of peroxisomes with anti-THI antibodies, whereas the *pex20-1* and *pex20KO* strains showed a diffuse pattern of staining characteristic of the cytosol (Fig. 8 *A*, *leftmost panels*). Anti-MLS and anti-SKL antibodies (Fig. 8 *A*, *middle panels*), or anti-Pex2p and anti-SKL antibodies (Fig. 8 *A*, *rightmost panels*), revealed a punctate pattern of staining in wild-type, *pex20-1,* and *pex20KO* cells. These data support the conclusion that mutations in the *PEX20* gene abolish THI import into peroxisomes but not the import of other peroxisomal matrix and membrane proteins. It is interesting to note that most cells of the *pex20-1* and *pex20KO* strains contained up to 20% of peroxisomes that were decorated by anti-MLS or anti-Pex2p antibodies, but not by anti-SKL antibodies (Fig. 8 *B*, *arrows*). Similarly decorated punctate structures were rarely observed in wild-type cells. Anti-MLS and anti-Pex2p antibodies always colocalized in punctate structures in wild-type, *pex20-1,* and *pex20KO* cells (Fig. 8 *B*, *rightmost panels*, data for *pex20KO* cells; data for wild-type and *pex20-1* cells is not shown). Therefore, wild-type cells apparently accumulate a few peroxisomes containing both MLS and Pex2p but not anti-SKL–reactive proteins, and mutations in the *PEX20* gene significantly increase the number of this type of peroxisome. These data, combined with EM results presented above showing a large increase in very small peroxisomes in *pex20* cells versus wild-type cells; the selective enrichment in the 200KgP of MLS, CAT, Pex2p, and Pex16p; and the decreased rate and efficiency of transit of MLS, Pex2p, and Pex16p from the 200KgP to the 20KgP, suggest that mutations in the *PEX20* gene lead to a large increase in very small peroxisomes that are enriched for MLS, CAT, Pex2p, and Pex16p. The role that Pex20p might play in the accumulation of very small HSP peroxisomes enriched for these proteins is currently under investigation.

Association of Pex20p with Newly Synthesized Thiolase in the Cytosol Is Not Dependent on the PTS2 of Thiolase

Our data showing that (*a*) most Pex20p is localized to the cytosol, (*b*) Pex20p apparently shuttles between the cytosol and the cytosolic surface of HSP peroxisomes, and (*c*) Pex20p is essential for the import of THI from the cytosol into HSP peroxisomes, led to a prediction that Pex20p and THI form a complex in the cytosol. To test this prediction, pulse-labeled Pex20p and THI were immunoprecipitated from the 200KgS (cytosolic) fraction of the wild-type strain under native conditions. Both anti-Pex20p and anti-THI antibodies immunoprecipitated two radiolabeled proteins with molecular weights of 59.8 and 47.0 kD, which could be decorated with anti-Pex20p and anti-THI antibodies, respectively (Fig. 9 *A*, *panels 1* and *6*). Therefore, Pex20p and THI form a complex in the cytosol of wild-type cells. Proteins that did not bind to protein A–Sepharose and were recovered in the flow-through following native (first) immunoprecipitation with anti-Pex20p or anti-THI antibodies were subjected to a second immunoprecipitation under denaturing conditions with anti-

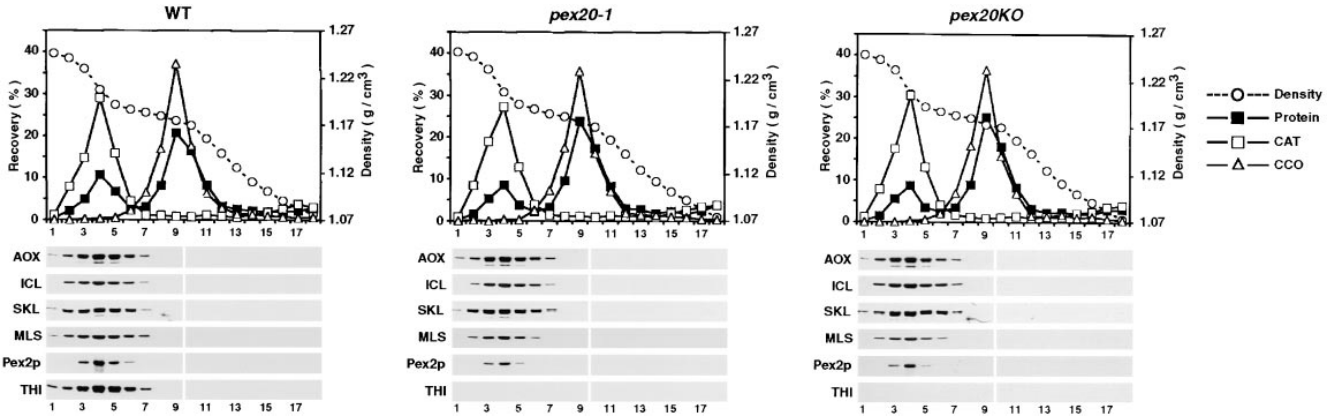

Figure 7. Isolation of LSP peroxisomes from wild-type and mutant strains. Wild-type strain *E122* (*WT*) and mutant strains *pex20-1* and *pex20KO* were grown in YPBO. Peroxisomes were isolated from the 20KgP of each strain by isopycnic centrifugation on a discontinuous sucrose density gradient. Equal amounts of protein were loaded onto each gradient. Sucrose density (g/cm^3) of gradient fractions, and the percent recovery of loaded protein and of CAT (peroxisome) and cytochrome *c* oxidase (*CCO*) (mitochondria) marker enzyme activities in gradient fractions are presented. Equal volumes of gradient fractions were analyzed by immunoblotting with antibodies to peroxisomal matrix (*AOX*, *ICL*, *SKL*, *MLS*, *THI*) and membrane (*Pex2p*) proteins.

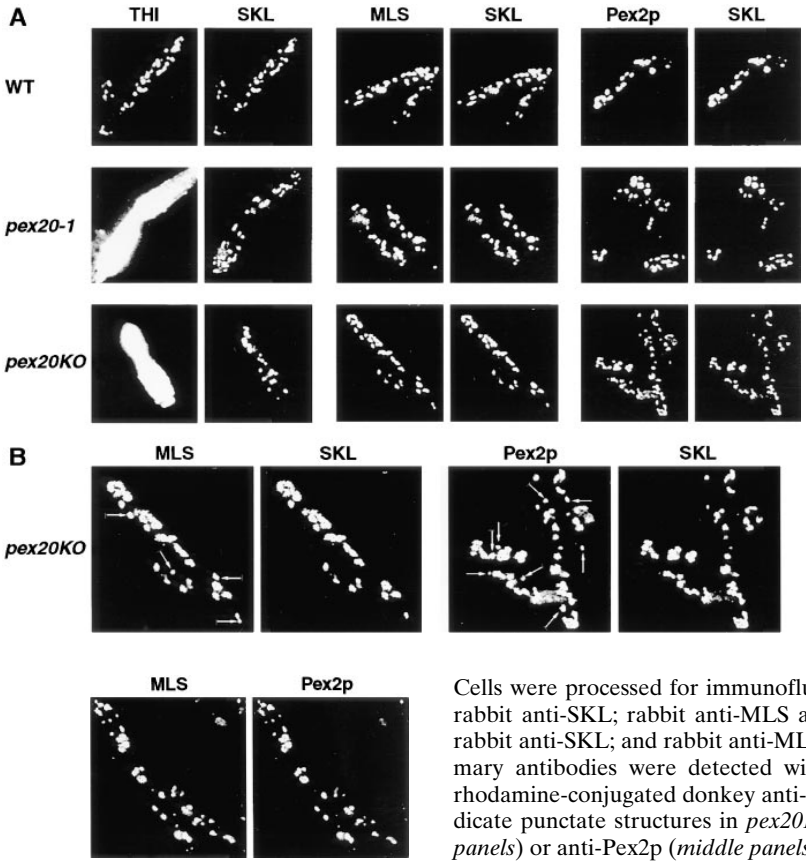

Figure 8. Double-labeling, indirect immunofluorescence analysis of wild-type and mutant strains. Wild-type strain *E122* (*WT*) and mutant strains *pex20-1* and *pex20KO* were grown in YPBO. Cells were processed for immunofluorescence microscopy with guinea pig anti-THI and rabbit anti-SKL; rabbit anti-MLS and guinea pig anti–SKL; guinea pig anti-Pex2p and rabbit anti-SKL; and rabbit anti-MLS and guinea pig anti-Pex2p primary antibodies. Primary antibodies were detected with fluorescein-conjugated goat anti-rabbit IgG and rhodamine-conjugated donkey anti-guinea pig IgG secondary antibodies. *Arrows* in *B* indicate punctate structures in *pex20KO* cells that are decorated with anti-MLS (*leftmost panels*) or anti-Pex2p (*middle panels*) antibodies but not with anti-SKL antibodies.

Pex20p or anti-THI antibodies. Neither Pex20p nor THI was recovered in the flow-through when the native immunoprecipitation had been performed with anti-Pex20p antibodies (Fig. 9 *A*, *panels 2* and *3*, respectively). Therefore, all newly synthesized THI was associated with Pex20p in the cytosol of wild-type cells. On the other hand, a significant portion of Pex20p, but no THI, was recovered in the flow-through when the native immunoprecipitation had been performed with anti-THI antibodies (Fig. 9 *A*, *panels 7* and *8*, respectively). Therefore, in the cytosol of wild-type cells, Pex20p is present in two forms, namely associated or unassociated with newly synthesized THI. Newly synthesized 62-kD SKL, 64-kD SKL, and MLS were not associated with either Pex20p or THI in the cytosol of wild-type cells, since none of these proteins was coimmunoprecipitated by anti-Pex20p (Fig. 9 *A*, *panels 1*, *4*, and *5*) or anti-THI (Fig. 9 *A*, *panels 6*, *9*, and *10*) antibodies under native conditions. Native immunoprecipitation using anti-SKL antibodies did not lead to coimmunoprecipitation of Pex20p, THI, or MLS with 62-kD SKL and 64-kD SKL proteins (Fig. 9 *A*, *panels 11–15*).

We tested whether the cleaved PTS2 of THI is essential for Pex20p binding. Only the precursor form of THI (pTHI) accumulates in peroxisomes of the *pex5KO* mutant deficient in the PTS1 import receptor (Fig. 9 *B*) (Szilard et al., 1995), whereas wild-type peroxisomes contain only the mature (mTHI) form of THI lacking its PTS2 (Fig. 9 *B*). Radiolabeled pTHI and mTHI forms were purified from peroxisomes of *pex5KO* and wild-type cells, respectively, and used as probes in a blot overlay assay with unlabeled proteins of either the cytosol of wild-type cells containing Pex20p (refer to Fig. 2 *A*) or the cytosols of

Figure 9. The association of Pex20p with newly synthesized THI in the cytosol is independent of the PTS2 of THI. (*A*) Wild-type *E122* cells grown in YPBO for 9 h were pulse-labeled with L-[^{35}S]methionine for 1.5 min and immediately subjected to subcellular fractionation to yield a 200KgS (cytosolic) fraction. The 200KgS fraction was divided into three equal aliquots, and Pex20p (*1*), THI (*6*), and anti-SKL–reactive proteins (*11*) were immunoprecipitated under native conditions. Immunoprecipitated proteins were eluted from protein A–Sepharose with 100 mM glycine, pH 2.8, and eluates were each divided into equal aliquots that were resolved by SDS-PAGE. One aliquot was subjected to fluorography, whereas the other four were analyzed by immunoblotting with anti-Pex20p, anti-THI, anti-SKL, or anti-MLS antibodies. Unbound proteins recovered in the flow-through after native immunoprecipitation with anti-Pex20p, anti-THI, and anti-SKL antibodies were subjected to a second immunoprecipitation under denaturing conditions using anti-Pex20p (*2*, *7*, *12*), anti-THI (*3*, *8*, *13*), anti-SKL (*4*, *9*, *14*) or anti-MLS (*5*, *10*, *15*) antibodies. Immunoprecipitates were divided into equal aliquots that were resolved by SDS-PAGE. One aliquot was subjected to fluorography, whereas the other four were analyzed by immunoblotting using the antibodies indicated. (*B*) The wild-type strain *E122* and the mutant strain *pex5KO* grown in YPBO for 9 h were pulse labeled with L-[^{35}S]methionine and chased for 30 min with unlabeled L-methionine. Cells were subjected to subcellular fractionation and peroxisomes were purified from the 20KgP fraction. Pulse-labeled and chased peroxisomal matrix proteins were subjected to immu-

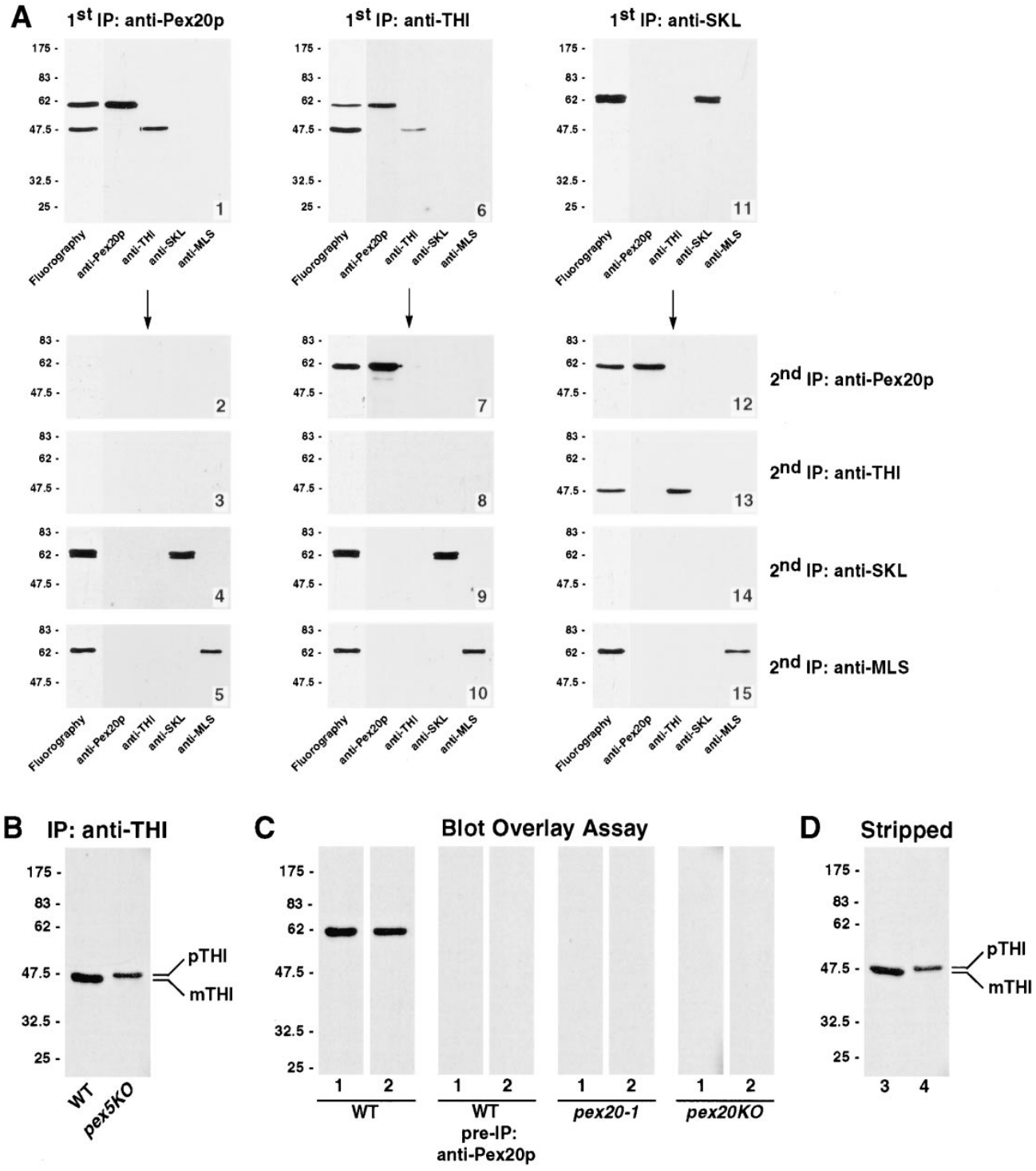

noaffinity chromatography with anti-THI antibodies linked to protein A–Sepharose. Immunoprecipitated mature (*mTHI*) and precursor (*pTHI*) forms of THI were eluted with 100 mM glycine, pH 2.8, and the eluates were divided into equal aliquots. One aliquot of each eluate was resolved by SDS-PAGE and subjected to fluorography (*B*), whereas the other aliquots were used as probes in a blot overlay assay. (*C*) Unlabeled proteins from the 200KgS fraction of wild-type cells were divided into equal aliquots. One aliquot was subjected to depletion of Pex20p by native immunoprecipitation with Pex20p antibodies (*pre-IP: anti-Pex20p*), whereas the second aliquot remained untreated. Unbound cytosolic proteins recovered in the flow-through after native immunoprecipitation with anti-Pex20p, unlabeled proteins from the untreated 200KgS fraction of wild-type cells, and unlabeled proteins from the 200KgS fractions of *pex20-1* and *pex20KO* cells were divided into equal aliquots, resolved by SDS-PAGE, and transferred to nitrocellulose. After denaturation/renaturation of the transferred proteins, the blots were subjected to an overlay assay using mTHI (*strips 1*) or pTHI (*strips 2*) as probes. One set of blots was subjected to fluorography (*C*), whereas a second set was used for stripping of bound mTHI and pTHI with urea (*D*). (*D*) Radiolabeled mTHI and pTHI (lanes *3* and *4*, respectively) bound to proteins present only in the untreated 200KgS fraction of the wild-type strain and stripped with urea, were resolved by SDS-PAGE and subjected to fluorography.

pex20-1 and *pex20KO* cells lacking Pex20p (refer to Fig. 2 *A*). Both pTHI and mTHI bound with equal efficiency to a 59.8-kD protein present in the cytosol of wild-type cells but absent in the cytosols of *pex20-1* or *pex20KO* cells (Fig. 9 *C*). Neither pTHI nor mTHI interacted with any protein when the wild-type cytosol was depleted of Pex20p by native immunoprecipitation with anti-Pex20p antibodies (Fig. 9 *C*). Stripping of the proteins bound to the wild-type cytosol confirmed the binding of pTHI and mTHI (Fig. 9 *D*). These data indicate that the association of Pex20p with newly synthesized THI in the cytosol of wild-type cells is not dependent on the presence of a PTS2 in THI.

Peroxisomal Pex20p and Thiolase Do Not Form a Complex

We tested whether THI remains associated with Pex20p after targeting of their complex from the cytosol to HSP peroxisomes. Proteins pulse labeled and chased for 5 min were immunoprecipitated from the 200KgP fraction of the wild-type strain under native conditions with anti-Pex20p or anti-THI antibodies. Proteins that did not bind to protein A–Sepharose and were recovered in the flow-through were subjected to a second immunoprecipitation under denaturing conditions with anti-Pex20p or anti-THI antibodies. No coimmunoprecipitation of Pex20p and THI was seen with either anti-Pex20p or anti-THI antibodies (Fig. 10, *panels 1–3* and *6–8*). Therefore, Pex20p and THI associated with HSP peroxisomes do not form a complex with each other. This finding is in agreement with the results of protease protection experiments showing that Pex20p associated with the 200KgP is a peripheral membrane protein bound to the cytosolic surface of HSP peroxisomes, whereas THI is located exclusively in the matrix of HSP peroxisomes (refer to Figs. 2 *H* and 3 *B*). 62-kD SKL, 64-kD SKL, and MLS associated with HSP peroxisomes also did not coimmunoprecipitate with either Pex20p or THI (Fig. 10, *panels 1*, *4–6*, *9*, and *10*). Therefore, none of the matrix proteins tested associated with each other or with Pex20p in HSP peroxisomes.

pex20 Mutations Affect Thiolase Oligomerization in the Cytosol and Prevent the Formation of a Heterotetrameric Complex between Thiolase and Pex20p

As shown above, all newly synthesized THI is associated with Pex20p in the cytosol of wild-type cells. We studied the oligomeric state of THI and of the complex formed between THI and Pex20p in wild-type cytosol by chemical cross-linking. The 200KgS (cytosolic) fraction of oleic acid-grown wild-type cells pulse-labeled with L-[^{35}S]methionine was subjected to increasing concentrations of the noncleavable, amine-reactive, homobifunctional cross-linker DSS. Proteins were immunoprecipitated under denaturing conditions with anti-THI antibodies, and proteins that did not bind to protein A–Sepharose and were recovered in the flow-through were subjected to a second immunoprecipitation under denaturing conditions with anti-Pex20p antibodies. SDS-PAGE analysis of cross-linked radiolabeled proteins immunoprecipitated with anti-THI antibodies revealed a 217-kD complex whose amount increased with increasing DSS, and a 47-kD (monomeric)

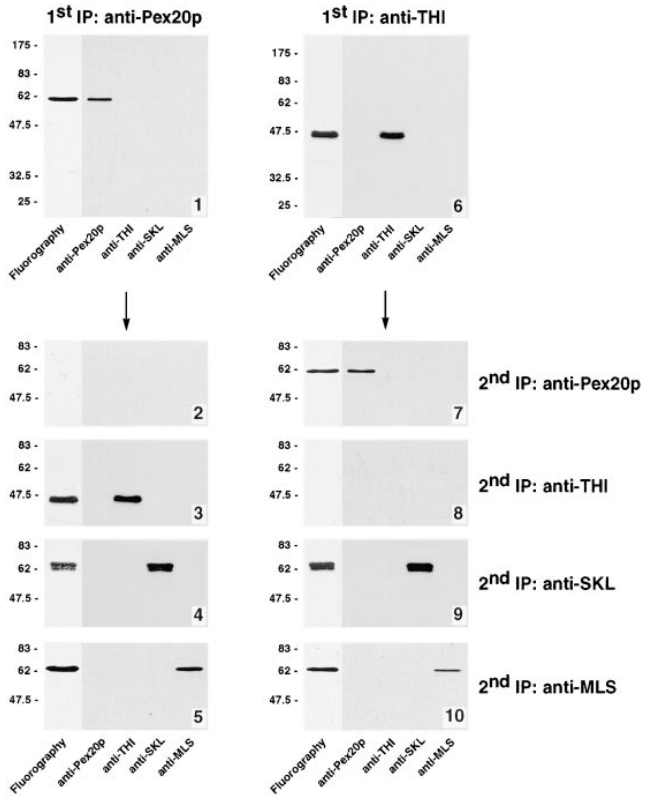

Figure 10. Pex20p and THI in the 200KgP fraction do not form a complex. Wild-type *E122* cells grown in YPBO for 9 h were pulse labeled with L-[^{35}S]methionine and chased for 5 min with unlabeled L-methionine. Cells were subjected to subcellular fractionation, and the 200KgP fraction was divided into equal aliquots that were subjected to immunoprecipitation under native conditions with anti-Pex20p (*1*) or anti-THI (*6*) antibodies. Proteins that did not bind to protein A–Sepharose and were recovered in the flow-through after native immunoprecipitation with either anti-Pex20p or anti-THI antibodies were subjected to a second immunoprecipitation under denaturing conditions using anti-Pex20p (*2*, *7*), anti-THI (*3*, *8*), anti-SKL (*4*, *9*) or anti-MLS (*5*, *10*) antibodies. These immunoprecipitates were resolved by SDS-PAGE and were analyzed by fluorography and immunoblotting with the indicated antibodies.

form of THI that concomitantly decreased and eventually disappeared (Fig. 11 *A*). Immunoprecipitation of Pex20p from the flow-through of the first immunoprecipitation with anti-THI antibodies showed that as the concentration of DSS increased, the level of unbound Pex20p decreased (Fig. 11 *B*). Immunoprecipitation of cytosolic proteins with anti-Pex20p antibodies revealed that as the DSS concentration increased, a prominent 217-kD complex appeared and increased (Fig. 12 *B*). The electrophoretic mobility of this complex was identical to that of the 217-kD complex immunoprecipitated with anti-THI antibodies when samples were separated on the same gel (data not shown). Immunoprecipitation of THI from the protein A–Sepharose flow-through after immunoprecipitation with anti-Pex20p antibodies showed that as the DSS concentration increased, unbound, monomeric THI decreased and eventually disappeared (Fig. 11 *D*). Taken together, these data indicate that in wild-type cytosol, all newly synthe-

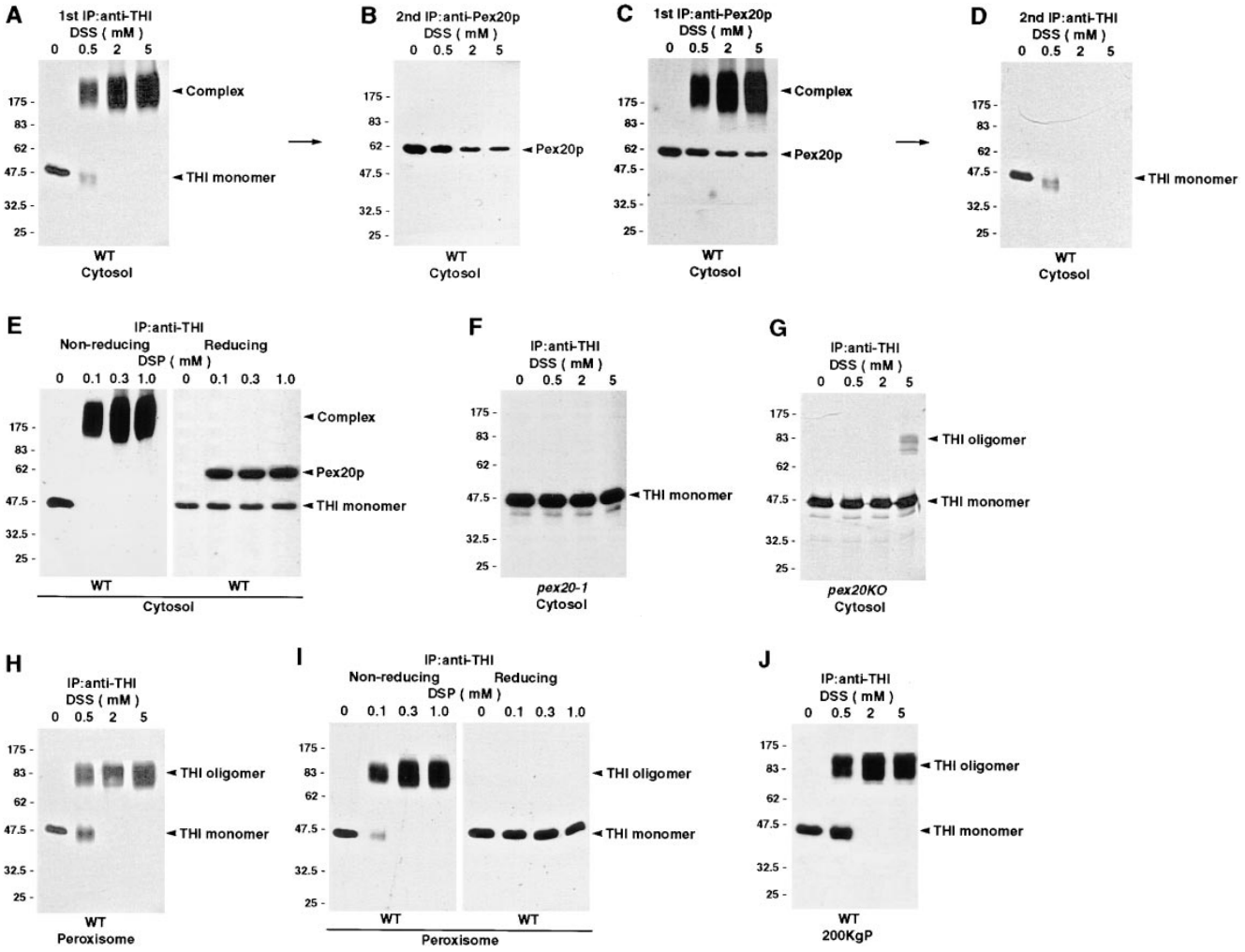

Figure 11. Mutations in the *PEX20* gene affect oligomerization of THI in the cytosol and prevent the formation of a heterotetrameric complex between Pex20p and THI. Wild-type strain *E122* and mutant strains *pex20-1* and *pex20KO* grown in YPBO for 9 h were pulse labeled with L-[^{35}S]methionine for 1.5 min and chased with unlabeled L-methionine. 200KgS (cytosolic) fractions were isolated from each strain at chase time 0. A 200KgP fraction (*200KgP*) enriched for HSP peroxisomes was isolated from wild-type cells chased for 7 min. LSP peroxisomes (*Peroxisome*) were isolated from the 20KgP of wild-type cells chased for 30 min. Cytosolic and peroxisomal proteins were treated with increasing concentrations of the cross-linkers DSS (*A–D, F–H, J*) or DSP (*E, I, K*) and subjected to immunoprecipitation with anti-THI (*A, E, F–K*) or anti-Pex20p (*C*) antibodies under denaturing conditions. Immunoprecipitates were resolved by SDS-PAGE and subjected to fluorography. Proteins that did not bind to protein A–Sepharose during immunoprecipitation of DSS-treated cytosolic proteins from wild-type cells with anti-THI (*A*) or anti-Pex20p (*C*) antibodies, were further immunoprecipitated with anti-Pex20p (*B*) or anti-THI (*D*) antibodies under denaturing conditions. Immunoprecipitates were resolved by SDS-PAGE and subjected to fluorography. Immunoprecipitated proteins treated with the noncleavable crosslinker DSS were analyzed by SDS-PAGE only under reducing conditions (*A–D, F–H, J*), whereas immunoprecipitated proteins treated with the thiol-cleavable cross-linker DSP were analyzed by SDS-PAGE under both nonreducing (*E, I, K*, *left panels*) and reducing (*E, I, K, right panels*) conditions. The positions of the monomeric and oligomeric forms of THI, of the monomeric form of Pex20p, and of the complex between Pex20p and THI are indicated by arrowheads (*right*).

sized THI and a significant portion of Pex20p are components of a 217-kD complex. The fact that only THI and Pex20p can be coimmunoprecipitated under native conditions with either anti-THI or anti-Pex20p antibodies (refer to Fig. 9 *A*) suggests that they are the only protein components of the 217-kD complex. That this was the case was confirmed by experiments using the thiol-cleavable, homobifunctional cross-linker DSP. Treatment of cytosolic proteins with increasing concentrations of DSP, followed by immunoprecipitation with anti-THI antibodies and evaluation of radiolabeled proteins by nonreducing SDS-PAGE and fluorography, showed that even at low concentrations of DSP, a 217-kD complex appeared, whereas there was concomitant disappearance of 47-kD

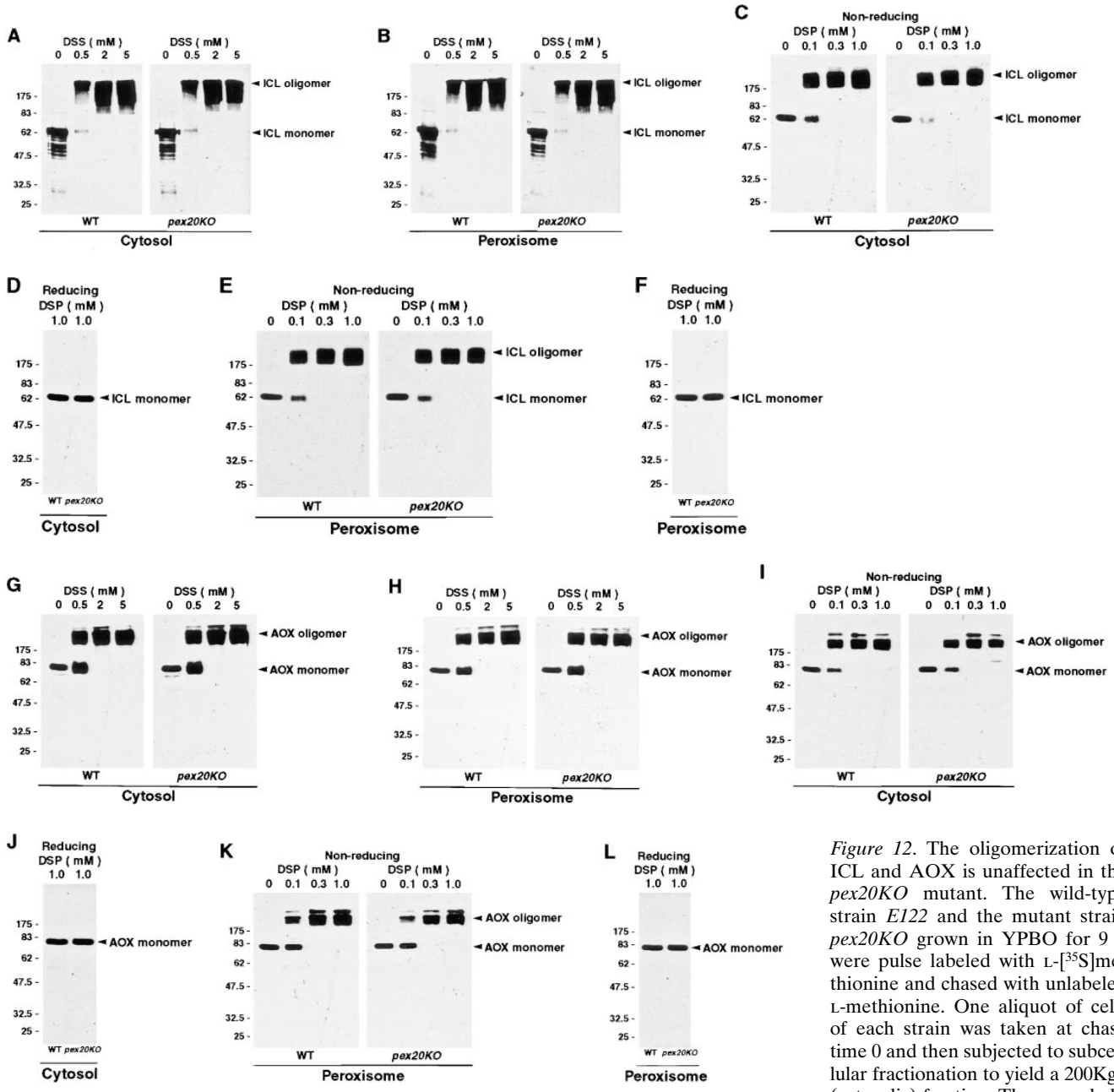

Figure 12. The oligomerization of ICL and AOX is unaffected in the *pex20KO* mutant. The wild-type strain *E122* and the mutant strain *pex20KO* grown in YPBO for 9 h were pulse labeled with L-[^{35}S]methionine and chased with unlabeled L-methionine. One aliquot of cells of each strain was taken at chase time 0 and then subjected to subcellular fractionation to yield a 200KgS (cytosolic) fraction. The second aliquots of the wild-type and *pex20KO* mutant cells were chased for 30 min, and LSP peroxisomes were isolated from the 20KgP fraction. Cytosolic and peroxisomal proteins were treated with increasing concentrations of the crosslinkers DSS (*A*, *B*, *G*, and *H*) or DSP (*C–F*, *I–L*) and subjected to immunoprecipitation with anti-ICL (*A–F*) or anti-AOX (*G–L*) antibodies under denaturing conditions. Immunoprecipitates were resolved by SDS-PAGE and subjected to fluorography. Immunoprecipitated proteins treated with the noncleavable crosslinker DSS were analyzed by SDS-PAGE only under reducing conditions (*A*, *B*, *G*, and *H*). Immunoprecipitated proteins treated with the thiol-cleavable cross-linker DSP were analyzed by SDS-PAGE under nonreducing (*C*, *E*, *I*, and *K*) and reducing (*D*, *F*, *J*, and *L*) conditions. The positions of the monomeric and oligomeric forms of ICL and AOX are indicated by arrowheads (*right*).

monomeric THI (Fig. 11 *E*, *left*). When DSP was cleaved with DTT, and the immunoprecipitated proteins were resolved by SDS-PAGE under reducing conditions, only two proteins of 59.8 and 47.0 kD were detected in the samples treated with DSP (Fig. 11 *E*, *right*). To quantitate the stoichiometry of Pex20p and THI in the 217-kD complex, the densities of the signals for Pex20p and THI in Fig. 11 *E*, *right*, *lane 1.0* were divided by 17 and 8, respectively, the number of methionine residues in Pex20p and THI, respectively. The ratio obtained was 1.1 ± 0.1 (data from four independent experiments), indicating that Pex20p and THI are present in equimolar amounts in the complex. Based on this observation and on a consideration of the molecular weights of Pex20p, pTHI, and the complex formed by these two proteins (59.8-, 47.0-, and 217-kD, respectively), we conclude that in the cytosol of wild-type

cells, all newly synthesized THI is associated with Pex20p in a heterotetrameric complex composed of two polypeptide chains of each protein.

We also tested the effects of the *pex20-1* and *pex20KO* mutations on the oligomerization of THI in the cytosol. Interestingly, most THI in the cytosol of *pex20* mutants is present as the monomeric form, even at the highest concentration of DSS (Fig. 11, *F* and *G*). Therefore, mutations in the *PEX20* gene affect oligomerization of newly synthesized THI in the cytosol and prevent the formation of the heterotetrameric complex between Pex20p and THI.

We also evaluated the oligomeric state of mature THI in LSP and HSP peroxisomes of oleic-acid grown wild-type cells. Both forms of peroxisomes were treated with increasing concentrations of DSS or DSP and then subjected to immunoprecipitation with anti-THI antibodies. Treatment of DSS cross-linked proteins under reducing conditions and DSP cross-linked proteins under nonreducing conditions revealed a prominent 86-kD protein that increased with increasing concentration of cross-linker (Fig. 11, *H* and *J*, and *I* and *K* [*left panels*]). No monomeric THI was detected in either LSP or HSP peroxisomes in samples treated with the highest concentration of cross-linker. On the other hand, only monomeric THI was seen in DSP-treated samples cleaved with DTT and analyzed by SDS-PAGE under reducing conditions (Fig. 11, *I* and *K*, *right panels*). From these data, we conclude that the mature form of THI is present exclusively as a homodimer in LSP and HSP peroxisomes of the wild-type strain.

Mutations in the PEX20 Gene Do Not Affect the Oligomerization of Isocitrate Lyase and Acyl-CoA Oxidase in the Cytosol

Chemical cross-linking of pulse-labeled proteins, followed by the immunoprecipitation with anti-ICL or anti-AOX antibodies, was used to study the oligomeric state of ICL and AOX in the cytosol and in peroxisomes of the wild-type and *pex20* mutant strains. Treatment with increasing concentrations of either DSS or DSP showed that ICL and AOX were present primarily as complexes rather than as monomers in the 200KgS (cytosolic) fraction (Fig. 12, *A*, *C*, *G,* and *I*), in LSP peroxisomes (Fig. 12, *B*, *E*, *H*, and *K*) and in HSP peroxisomes (data not shown) of the wild-type strain. The electrophoretic mobilities of ICL- and AOX-containing complexes from the cytosol were identical to those from LSP and HSP peroxisomes when resolved by SDS-PAGE on the same gel (data not shown). DTT treatment and reducing SDS-PAGE analysis of DSP cross-linked samples showed that only the monomeric forms of ICL and AOX could be recovered from cytosol (Fig. 12, *D* and *J*), LSP peroxisomes (Fig. 12, *F* and *L*) and HSP peroxisomes (data not shown) of the wild-type strain. The oligomerization of ICL or AOX was unaffected in both the *pex20-1* and *pex20K*O mutants (Fig. 12, data for the *pex20KO* strain; data for the *pex20-1* strain not shown). From these data, we conclude that newly synthesized ICL and AOX rapidly oligomerize in the cytosol of wild-type cells and are imported into peroxisomes as homooligomers. Mutations in the *PEX20* gene do not affect the formation of the homooligomers of ICL and AOX in the cytosol and do not impair their subsequent import into peroxisomes.

Discussion

Oligomerization of Thiolase in the Cytosol Is a Prerequisite for Its Targeting to the Peroxisome

Our kinetic data show that the oligomerization of THI in the cytosol precedes its import into the peroxisome. At the end of a short pulse with radiolabeled methionine, all labeled THI was found exclusively in a cytosolic heterotetrameric complex of two THI and two Pex20p polypeptide chains. Labeled THI was chased to peroxisomes and was imported exclusively as a homodimer. Mutations in the *PEX20* gene not only affected the oligomerization of THI in the cytosol but also abolished import of THI into peroxisomes. Two interpretations for the observed effects of *pex20* mutations on the oligomerization and peroxisomal targeting of THI can be proposed. First, Pex20p could be required only for the oligomerization and maintenance of the import-competent oligomeric state of THI and, therefore, oligomerization of THI in the cytosol not only precedes but is also required for its targeting to the peroxisome. Second, Pex20p could not only act as a cytosolic chaperone assisting oligomerization of THI in the cytosol, but could also function as a cytosolic THI import receptor that interacts with a specific docking site(s) on the peroxisomal membrane, thereby mediating docking of THI to the peroxisome.

Our data also show that not only THI, which contains a PTS2, but also ICL, which is targeted by PTS1 (Barth and Scheuber, 1993), and AOX, which lacks any conserved variant of PTS1 or PTS2 (Nicaud et al., 1988), are imported into peroxisomes of *Y. lipolytica* as oligomers. Our results extend recent observations that peroxisomes can translocate folded, disulfide-bonded and oligomeric proteins, and even 9-nm colloidal gold particles, across their membranes (Glover et al., 1994*a*; McNew and Goodman, 1994; Walton et al., 1995; Elgersma et al., 1996; Häusler et al., 1996; Leiper et al., 1996; Lee et al., 1997). Although polypeptide chains lacking a PTS can be translocated into the peroxisomal matrix in a piggyback fashion on PTS1- and PTS2-containing proteins (for review see Rachubinski and Subramani, 1995; McNew and Goodman, 1996; Subramani, 1998), we did not see evidence of piggybacking of THI, ICL, or AOX into the peroxisomal matrix in *Y. lipolytica*. According to our data, THI penetrates the peroxisome exclusively as a homodimer rather than as a component of a cytosolically formed heterotetrameric complex of THI and Pex20p. Our data also show that newly synthesized ICL and AOX rapidly homooligomerize in the cytosol and are imported as homooligomers, which suggests that they are not piggybacked into peroxisomes.

Pex20p May Act As a Cytosolic Chaperone Assisting Thiolase Oligomerization

Mutations in the *PEX20* gene abolish the assembly of newly synthesized monomers of THI into a heterotetrameric complex of THI and Pex20p, suggesting that Pex20p may act as a cytosolic chaperone that assists in the oligomerization of THI in vivo. Molecular chaperones were originally defined as temporary partners that assist in the oligomeric assembly of unassembled subunits of oligomeric proteins (for review see Hendrick and Hartl, 1993).

Our results indicate that two polypeptides of Pex20p bind temporarily to two polypeptide chains of THI and that this heterotetrameric complex dissociates upon binding to the outer surface of the peroxisomal membrane, releasing THI homodimer into the peroxisomal matrix. Moreover, since oligomerization of THI in the cytosol (see above) is a prerequisite for its targeting to the peroxisome, we propose that Pex20p acts as a putative cytosolic chaperone to maintain the import-competent oligomeric state of THI. Our data also show that the substrate specificity of Pex20p as a putative cytosolic chaperone is limited to THI. Pex20p does not bind the newly synthesized cytosolic form of any peroxisomal protein other than THI, and it is not essential for the targeting of any peroxisomal protein other than THI from the cytosol to the peroxisome nor is it required for the oligomeric assembly of ICL and AOX in the cytosol. Pex20p is also apparently not required for the folding of newly synthesized monomers of THI in the cytosol, as our results show that newly synthesized monomeric THI is enzymatically active (data not shown), does not form insoluble aggregates and is not degraded in the cytosol of the *pex20* mutant strains. This step of THI maturation in the cytosol may be assisted by other cytosolic chaperone(s) such as TRiC (TCP1 ring complex), the eukaryotic homologue of GroEL (for review see Horwich and Willison, 1993; Bukau et al., 1996; Hartl, 1996), or cytosolic Hsp70. TriC has been shown to assist in the folding of the peroxisomal matrix protein, firefly luciferase (Frydman et al., 1994; Frydman and Hartl, 1996), and to bind to the peroxisomal membrane protein, PMP22 (Pause et al., 1997). Cytosolic Hsp70 also binds to firefly luciferase (Frydman et al., 1994; Frydman and Hartl, 1996) and has been shown to play an essential role in peroxisomal protein import (Walton et al., 1994).

A Model for Pex20p-mediated Oligomerization and Peroxisomal Import of Thiolase

The results of this study can be summarized in the following model for Pex20p-assisted oligomerization and peroxisomal import of THI. Monomeric Pex20p binds newly synthesized monomeric THI in the cytosol and promotes the formation of a heterotetrameric complex composed of two polypeptide chains of each protein. The association of Pex20p with THI is independent of the PTS2 in THI. The heterotetrameric complex binds to the peroxisomal membrane. Translocation of the THI homodimer into the peroxisomal matrix may release Pex20p monomers back to the cytosol, thereby permitting a new cycle of binding-oligomerization-targeting-release for Pex20p and THI. Binding of Pex20p to THI is PTS2 independent because, as we have shown, Pex20p interacts with PTS2-containing and PTS2-lacking forms of THI with equal efficiency. No receptor that binds PTS2 directly and is required for import of PTS2-containing THI has yet been identified in *Y. lipolytica*. However, PTS2 receptors of the Pex7p peroxin family have been identified in *S. cerevisiae* (Marzioch et al., 1994; Zhang and Lazarow, 1995, 1996; Rehling et al., 1996), *Kluyveromyces lactis* (Motley et al., 1997), *Pichia pastoris* (Elgersma et al., 1998), mouse (Braverman et al., 1997) and human (Braverman et al., 1997; Motley et al., 1997; Purdue et al., 1997). The exact subcellular location of the PTS2 receptor is a matter of debate and has been reported as mainly cytosolic and partially peroxisomal (Marzioch et al., 1994; Rehling et al., 1996) or exclusively intraperoxisomal (Zhang and Lazarow, 1995, 1996). Accordingly, two alternative models for PTS2 receptor action have been proposed. The first proposes that Pex7p is a mobile receptor, shuttling between the cytosol and the peroxisome (Marzioch et al., 1994; Rehling et al., 1996). The second proposes that Pex7p acts from within the peroxisome to pull THI inside the organelle and predicts the existence of another peroxin to interact with PTS2-containing THI, either in the cytosol or at the outer surface of the peroxisomal membrane (Zhang and Lazarow, 1995, 1996). Both models could accommodate the existence of a cytosolic peroxin such as Pex20p that not only maintains the oligomeric (import-competent) state of THI but which could also stabilize a conformation of THI that makes PTS2 more accessible to Pex7p. In the first model, cytosolic Pex20p could interact with a region of THI outside of the PTS2, whereas cytosolic Pex7p would bind the PTS2 directly. The cooperative action of Pex7p and Pex20p in the cytosol would permit correct targeting of THI to the peroxisomal docking protein Pex14p (Albertini et al., 1997), followed by translocation of THI into the matrix. In the second model, cytosolic Pex20p would maintain the oligomeric (import-competent) state of THI and could stabilize a conformation of THI that makes PTS2 more accessible to Pex7p, thereby mediating targeting of THI to the peroxisomal membrane. Subsequent interaction of intraperoxisomal Pex7p with an exposed PTS2 would initiate pulling of THI inside the organelle. It should be noted that in the blot overlay assay, no cytosolic protein other than Pex20p was seen to interact with pTHI or mTHI. The inability to detect a cytosolic PTS2 receptor that interacts only with pTHI but not with mTHI may be the result of Pex20p having a significantly higher affinity for pTHI than does any other cytosolic protein. An alternative explanation might be that the *Y. lipolytica* PTS2 receptor is exclusively intraperoxisomal. We are currently developing genetic screens aimed at identifying Pex7p of *Y. lipolytica* so as to critically evaluate both models in regards to a cooperative action of Pex7p and Pex20p in the peroxisomal import of THI.

In conclusion, the results described herein provide evidence that the oligomerization of THI in the cytosol requires the peroxin Pex20p and is a prerequisite for THI import into peroxisomes in *Y. lipolytica*. THI and Pex20p interact in a PTS2-independent manner and form a heterotetrameric cytosolic complex composed of two polypeptide chains of each protein. After targeting of the complex to the peroxisomal membrane, the homodimer of THI is translocated into the peroxisomal matrix, and Pex20p monomers are envisaged to recycle to the cytosol to permit a new cycle of binding-oligomerization-targeting-release between Pex20p and THI.

We thank H. Chan (University of Alberta, Edmonton, Alberta, Canada) for help with electron microscopy.

This work was supported by grant MT-9208 from the Medical Research Council (MRC) of Canada to R.A. Rachubinski. R.A. Rachubinski is an MRC Senior Scientist and an International Research Scholar of the Howard Hughes Medical Institute.

Received for publication 8 April 1998 and in revised form 9 June 1998.

References

Abeijon, C., P. Orlean, P.W. Robins, and C.B. Hirschberg. 1989. Topography of glycosylation in yeast: characterization of GDP-mannose transport and lumenal guanosine diphosphatase activities in Golgi-like vesicles. *Proc. Natl. Acad. Sci. USA*. 86:6935–6939.

Albertini, M., P. Rehling, R. Erdmann, W. Girzalsky, J.A.K.W. Kiel, M. Veenhuis, and W.-H. Kunau. 1997. Pex14p, a peroxisomal membrane protein binding both receptors of the two PTS-dependent import pathways. *Cell.* 89: 83–92.

Ausubel, F.J., R. Brent, R.E. Kingston, D.D. Moore, J.G. Seidman, J.A. Smith, and K. Struhl. 1989. *In* Current Protocols in Molecular Biology. Greene Publishing Associates, New York. 3.1–3.17, 13.11–13.12.

Barth, G., and T. Scheuber. 1993. Cloning of the isocitrate lyase gene (ICL1) from *Yarrowia lipolytica* and characterization of the deduced protein. *Mol. Gen. Genet.* 241:422–430.

Bellion, E., and J.M. Goodman. 1987. Proton ionophores prevent assembly of a peroxisomal protein. *Cell.* 48:165–173.

Boisramé, A., J.-M. Beckerich, and C. Gaillardin. 1996. Sls1p, an endoplasmic reticulum component, is involved in the protein translocation process in the yeast *Yarrowia lipolytica*. *J. Biol. Chem.* 271:11668–11675.

Braverman, N., G. Steel, C. Obie, A. Moser, H. Moser, S.J. Gould, and D. Valle. 1997. Human *PEX7* encodes the peroxisomal PTS2 receptor and is responsible for rhizomelic chondrodysplasia punctata. *Nat. Genet.* 15:369–376.

Bukau, B., T. Hesterkamp, and J. Luirink. 1996. Growing in a dangerous environment: a network of multiple targeting and folding pathways for nascent polypeptides in the cytosol. *Trends Cell Biol.* 6:480–486.

Coligan, J.E., B.M. Dunn, H.L. Ploegh, D.W. Speicher, and P.T Wingfield. 1995. *In* Current Protocols in Protein Science. Wiley Interscience, New York. 10.11.1–10.11.6.

Dingwall, C., S. Kandels-Lewis, and B. Séraphin. 1995. A family of Ran binding proteins that includes nucleoporins. *Proc. Natl. Acad. Sci. USA*. 92:7525–7529.

Distel, B., R. Erdmann, S.J. Gould, G. Blobel, D.I. Crane, J.M. Cregg, G. Dodt, Y. Fujiki, J.M. Goodman, W.W. Just, J.A.K.W. Kiel, W.-H. Kunau, P.B. Lazarow, G.P. Mannaerts, H. Moser, T. Osumi, R.A. Rachubinski, A. Roscher, S. Subramani, H.F. Tabak, D. Valle, I. van der Klei, P.P. van Veldhoven, and M. Veenhuis. 1996. A unified nomenclature for peroxisome biogenesis. *J. Cell Biol.* 135:1–3.

Dodt, G., and S.J. Gould. 1996. Multiple *PEX* genes are required for proper subcellular distribution and stability of Pex5p, the PTS1 receptor: evidence that PTS1 protein import is mediated by a cycling receptor. *J. Cell Biol.* 135: 1763–1774.

Eitzen, G.A., J.D. Aitchison, R.K. Szilard, M. Veenhuis, W.M. Nuttley, and R.A. Rachubinski. 1995. The *Yarrowia lipolytica* gene *PAY2* encodes a 42-kDa peroxisomal integral membrane protein essential for matrix protein import and peroxisome enlargement but not for peroxisome membrane proliferation. *J. Biol. Chem.* 270:1429–1436.

Eitzen, G.A., V.I. Titorenko, J.J. Smith, M. Veenhuis, R.K. Szilard, and R.A. Rachubinski. 1996. The *Yarrowia lipolytica* gene *PAY5* encodes a peroxisomal integral membrane protein homologous to the mammalian peroxisome assembly factor PAF-1. *J. Biol. Chem.* 271:20300–20306.

Eitzen, G.A., R.K. Szilard, and R.A. Rachubinski. 1997. Enlarged peroxisomes are present in oleic acid-grown *Yarrowia lipolytica* overexpressing the *PEX16* gene encoding an intraperoxisomal peripheral membrane peroxin. *J. Cell Biol.* 137:1265–1278.

Elgersma, Y., A. Vos, M. van den Berg, C.W. van Roermund, P. van der Sluijs, B. Distel, and H.F. Tabak. 1996. Analysis of the carboxyl-terminal peroxisomal targeting signal 1 in a homologous context in *Saccharomyces cerevisiae*. *J. Biol. Chem.* 271:26375–26382.

Erdmann, R., M. Veenhuis, and W.-H. Kunau. 1997. Peroxisomes: organelles at the crossroads. *Trends Cell Biol.* 7:400–407.

Elgersma, Y., M. Elgersma-Hooisma, T. Wenzel, J.M. McCaffery, M.G. Farquhar, and S. Subramani. 1998. A mobile PTS2 receptor for peroxisomal protein import in *Pichia pastoris*. *J. Cell Biol.* 140:807–820.

Franzusoff, A., J. Rothblatt, and R. Schekman. 1991. Analysis of polypeptide transit through yeast secretory pathway. *Methods Enzymol.* 194:662–674.

Frydman, J., and F.-U. Hartl. 1996. Principles of chaperone-assisted protein folding: differences between in vitro and in vivo mechanisms. *Science.* 272: 1497–1502.

Frydman, J., E. Nimmesgern, K. Ohtsuka, and F.-U. Hartl. 1994. Folding of nascent polypeptide chains in a high molecular mass assembly with molecular chaperones. *Nature.* 370:111–117.

Glover, J.R., D.W. Andrews, and R.A. Rachubinski. 1994*a*. *Saccharomyces cerevisiae* peroxisomal thiolase is imported as a dimer. *Proc. Natl. Acad. Sci. USA*. 91:10541–10545.

Glover, J.R., D.W. Andrews, S. Subramani, and R.A. Rachubinski. 1994*b*. Mutagenesis of the amino targeting signal of *Saccharomyces cerevisiae* 3-ketoacyl-CoA thiolase reveals conserved amino acids required for import into peroxisomes in vivo. *J. Biol. Chem.* 269:7558–7563.

Goodman, J.M., S.B. Tramp, H. Hang, and M. Veenhuis. 1990. Peroxisomes induced in *Candida Baden* by methanol, oleic acid and D-alanine vary in metabolic function but share common integral membrane proteins. *J. Cell Sci.* 97:193–204.

Hartl, F.-U. 1996. Molecular chaperones in cellular protein folding. *Nature.* 381: 571–580.

Hendrick, J.P., and F.-U. Hartl. 1993. Molecular chaperone functions of heat-shock proteins. *Annu. Rev. Biochem.* 62:349–384.

Häusler, T., Y. Stierhof, E. Wirtz, and C. Clayton. 1996. Import of DHFR hybrid protein into glycosomes in vivo is not inhibited by the folate-analogue aminopterin. *J. Cell Biol.* 132:311–324.

Horwich, A.L., and K.R. Willison. 1993. Protein folding in the cell: functions of two families of molecular chaperone, hsp60 and TF55-TCP1. *Phil. Trans. R. Soc. Lond.* 339:313–326.

Kunau, W.-H. 1998. Peroxisome biogenesis: from yeast to man. *Curr. Opin. Microbiol.* In press.

Kyhse-Andersen, J. 1984. Electroblotting of multiple gels: a simple apparatus without buffer tank for rapid transfer of proteins from polyacrylamide to nitrocellulose. *J. Biochem. Biophys. Methods.* 10:203–209.

Laemmli, U.K. 1970. Cleavage of structural proteins during the assembly of the head of bacteriophage T4. *Nature.* 227:680–685.

Lanzetta, P.A., L.J. Alvarez, P.S. Reinach, and O.A. Candia. 1979. An improved assay for nanomole amounts of inorganic phosphate. *Anal. Biochem.* 100:95–97.

Lee, M.S., R.T. Mullen, and R.N. Trelease. 1997. Oilseed isocitrate lyases lacking their essential type I peroxisomal targeting signal are piggybacked to glyoxysomes. *Plant Cell*. 9:185–197.

Leiper, J.M., P.B. Oatey, and C.J. Danpure. 1996. Inhibition of alanine:glyoxylate aminotransferase 1 dimerization is a prerequisite for its peroxisome-to-mitochondrion mistargeting in primary hyperoxaluria type 1. *J. Cell Biol.* 135:939–951.

Lopez, M.C., J.-M. Nicaud, H.B. Skinner, C. Vergnolle, J.C. Kader, V.A. Bankaitis, and C. Gaillardin. 1994. A phosphatidylinositol/phosphatidylcholine transfer protein is required for differentiation of the dimorphic yeast *Yarrowia lipolytica* from the yeast to the mycelial form. *J. Cell Biol.* 125:113–127.

Marshall, P.A., J.M. Dyer, M.E. Quick, and J.M. Goodman. 1996. Redox-sensitive homodimerization of Pex11p: a proposed mechanism to regulate peroxisomal division. *J. Cell Biol.* 135:123–137.

Marzioch, M., R. Erdmann, M. Veenhuis, and W.-H. Kunau. 1994. *PAS7* encodes a novel yeast member of the WD-40 protein family essential for import of 3-oxoacyl-CoA thiolase, a PTS2-containing protein, into peroxisomes. *EMBO (Eur. Mol. Biol. Organ.) J.* 13:4908–4918.

McNew, J.A., and J.M. Goodman. 1994. An oligomeric protein is imported into peroxisomes in vivo. *J. Cell Biol.* 127:1245–1257.

McNew, J.A., and J.M. Goodman. 1996. The targeting and assembly of peroxisomal proteins: some old rules do not apply. *Trends Biochem. Sci.* 21:54–58.

Motley, A., E. Hettema, E.M. Hogenhout, P. Brites, A.L.M.A. ten Asbroek, F.A. Wijburg, F. Baas, H. Heijmans, H.F. Tabak, R.J.A. Wanders, and B. Distel. 1997. Rhizomelic chondrodysplasia punctata is a peroxisomal targeting disease caused by a non-functional PTS2 receptor. *Nat. Genet.* 15:377–380.

Nicaud, J.-M., A. Le Clainche, M.-T. Le Dall, H. Wang, and C. Gaillardin. 1998. *Yarrowia lipolytica*, a yeast model for the genetic studies of hydroxy fatty acids biotransformation into lactones. *J. Mol. Catal. B Enzymatic.* 151: In press.

Nuttley, W.M., A.M. Brade, C. Gaillardin, G.A. Eitzen, J.R. Glover, J.D. Aitchison, and R.A. Rachubinski. 1993. Rapid identification and characterization of peroxisomal assembly mutants in *Yarrowia lipolytica*. *Yeast*. 9:507–515.

Pause, B., P. Diestelkötter, H. Heid, and W.W. Just. 1997. Cytosolic factors mediate protein insertion into the peroxisomal membrane. *FEBS (Fed. Eur. Biochem. Soc.) Lett.* 414:95–98.

Purdue, P.E., and P.B. Lazarow. 1994. Peroxisomal biogenesis: multiple pathways of protein import. *J. Biol. Chem.* 269:30065–30068.

Purdue, P.E., J.W. Zhang, M. Skoneczny, and P.B. Lazarow. 1997. Rhizomelic chondrodysplasia punctata is caused by deficiency of human Pex7p, a homologue of the yeast PTS2 receptor. *Nat. Genet.* 15:381–384.

Rachubinski, R.A., and S. Subramani. 1995. How proteins penetrate peroxisomes. *Cell.* 83:525–528.

Radu, A., M.S. Moore, and G. Blobel. 1995. The peptide repeat domain of nucleoporin Nup98 as a docking site in transport across the nuclear pore complex. *Cell*. 81:215–222.

Rehling, P., M. Marzioch, F. Niesen, E. Wittke, M. Veenhuis, and W.-H. Kunau. 1996. The import receptor for the peroxisomal targeting signal 2 (PTS2) in *Saccharomyces cerevisiae* is encoded by the *PAS7* gene. *EMBO (Eur. Mol. Biol. Organ.) J.* 15:2901–2913.

Roberts, C.J., C.K. Raymond, C.T. Yamashiro, and T.H. Stevens. 1991. Methods for studying the yeast vacuole. *Methods Enzymol.* 194:644–661.

Sanders, S.L., K.M. Whitfield, J.P. Vogel, M.D. Rose, and R.W. Schekman. 1992. Sec61p and BiP directly facilitate polypeptide translocation into the ER. *Cell.* 69:353–365.

Schatz, G., and B. Dobberstein. 1996. Common principles of protein translocation across membranes. *Science.* 271:1519–1526.

Smith, J.J., R.K. Szilard, M. Marelli, and R.A. Rachubinski. 1997. The peroxin Pex17p of the yeast *Yarrowia lipolytica* is associated peripherally with the peroxisomal membrane and is required for the import of a subset of matrix proteins. *Mol. Cell. Biol.* 17:2511–2520.

Subramani, S. 1998. Components involved in peroxisome import, biogenesis, proliferation, turnover, and movement. *Pharmacol. Rev.* 78:171–188.

Szilard, R.K., V.I. Titorenko, M. Veenhuis, and R.A. Rachubinski. 1995. Pay32p of the yeast *Yarrowia lipolytica* is an intraperoxisomal component of the matrix protein translocation machinery. *J. Cell Biol.* 131:1453–1469.

Thieringer, R., H. Shio, Y.S. Han, G. Cohen, and P.B. Lazarow. 1991. Peroxi-

somes in *Saccharomyces cerevisiae*: immunofluorescence analysis and import of catalase A into isolated peroxisomes. *Mol. Cell. Biol.* 11:510–522.

Titorenko, V.I., and R.A. Rachubinski. 1998. Mutants of the yeast *Yarrowia lipolytica* defective in protein exit from the endoplasmic reticulum are also defective in peroxisome biogenesis. *Mol. Cell. Biol.* 18:2789–2803.

Titorenko, V.I., G.A. Eitzen, and R.A. Rachubinski. 1996. Mutations in the *PAY5* gene of the yeast *Yarrowia lipolytica* cause the accumulation of multiple subpopulations of peroxisomes. *J. Biol. Chem.* 271:20307–20314.

Titorenko, V.I., D.M. Ogrydziak, and R.A. Rachubinski. 1997. Four distinct secretory pathways serve protein secretion, cell surface growth, and peroxisome biogenesis in the yeast *Yarrowia lipolytica*. *Mol. Cell. Biol.* 17:5210–5226.

Walton, P.A., M. Wendland, S. Subramani, R.A. Rachubinski, and W.J. Welch. 1994. Involvement of 70-kD heat-shock proteins in peroxisomal import. *J. Cell Biol.* 125:1037–1046.

Walton, P.A., P.E. Hill, and S. Subramani. 1995. Import of stably folded proteins into peroxisomes. *Mol. Biol. Cell* 6:675–683.

Waterham, H.R., K.A. Russell, Y. de Vries, and J.M. Cregg. 1997. Peroxisomal targeting, import, and assembly of alcohol oxidase in *Pichia pastoris*. *J. Cell Biol.* 139:1419–1431.

Zhang, J.W., C. Luckey, and P.B. Lazarow. 1993. Three peroxisome protein packaging pathways suggested by selective permeabilization of yeast mutants defective in peroxisome biogenesis. *Mol. Biol. Cell.* 4:1351–1359.

Zhang, J.W., and P.B. Lazarow. 1995. *PEB1* (*PAS7*) in *Saccharomyces cerevisiae* encodes a hydrophilic, intra-peroxisomal protein that is a member of the WD repeat family and is essential for the import of thiolase into peroxisomes. *J. Cell Biol.* 129:65–80.

Zhang, J.W., and P.B. Lazarow. 1996. Peb1p (Pas7p) is an intraperoxisomal receptor for the NH_2-terminal, type 2, peroxisomal targeting signal of thiolase: Peb1p itself is targeted to peroxisome by an NH_2-terminal peptide. *J. Cell Biol.* 132:325–334.